

COMBINATORICS OF THE ZETA MAP ON RATIONAL DYCK PATHS

CESAR CEBALLOS, TOM DENTON, AND CHRISTOPHER R. H. HANUSA

ABSTRACT. An (a, b) -Dyck path P is a lattice path from $(0, 0)$ to (b, a) that stays above the line $y = \frac{a}{b}x$. The zeta map is a curious rule that maps the set of (a, b) -Dyck paths onto itself; it is conjecturally bijective, and we provide progress towards proof of bijectivity in this paper, by showing that knowing $\zeta(P)$ and $\zeta(P^c)$ is enough to recover P .

Our method begets an area-preserving involution χ on the set of (a, b) -Dyck paths when ζ is a bijection, as well as a new method for calculating ζ^{-1} on classical Dyck paths. For certain nice (a, b) -Dyck paths we give an explicit formula for ζ^{-1} and χ and for additional (a, b) -Dyck paths we discuss how to compute ζ^{-1} and χ inductively.

We also explore Armstrong's skew length statistic and present two new combinatorial methods for calculating the zeta map involving lasers and interval intersections. We conclude with two possible routes to a proof that ζ is a bijection. Notably, we provide a combinatorial statistic δ that can be used to recursively compute ζ^{-1} . We show that δ is computable from $\zeta(P)$ in the Fuss-Catalan case and provide evidence that δ may be computable from $\zeta(P)$ in general.

1. INTRODUCTION

Let a and b be relatively prime positive integers and let $\mathfrak{D}_{a,b}$ be the set of (a, b) -Dyck paths, lattice paths P from $(0, 0)$ to (b, a) staying above the line $y = \frac{a}{b}x$. These paths are often called *rational Dyck paths* and they generalize the classical and well-studied *Dyck paths*.

We study a remarkable automorphism ζ on rational Dyck paths which has received considerable attention lately; this “zeta map” generalizes the map on standard Dyck paths discovered by Haiman in study of diagonal harmonics and q, t -Catalan numbers [Hag08]. Combinatorial definitions of q, t -statistics for classical Dyck paths were famously difficult to find, but were nearly simultaneously discovered by Haglund and Haiman. Interestingly, they discovered two *different* pairs of statistics: Haiman found area and dinv shortly after Haglund discovered bounce and area statistics. The zeta map was then uncovered, which satisfies $\text{bounce}(\zeta(P)) = \text{area}(P)$ and $\text{area}(\zeta(P)) = \text{dinv}(P)$.

Many details about the zeta map have been gathered and unified in a comprehensive article by Armstrong, Loehr, and Warrington [ALW14b], including progress on proving its bijectivity in certain cases such as $(a, am \pm 1)$ -Dyck paths [Loe05, GM14] (which is associated to the Fuss-Catalan numbers). The zeta map was shown to be a bijection in these special cases by way of a “bounce path” by which zeta inverse could be computed. However, constructing such a bounce path for the general (a, b) case remains elusive. Armstrong, Loehr, and Warrington showed that there is a much larger family of sweep maps (for which the zeta map is a special case) which extensive computational exploration suggests are also bijective. A construct of theirs upon which we have relied heavily is the notion of the *levels* of a lattice path.

Recent progress on the zeta map has been made in the case when $a = 3$ by Kaliszewski and Li [KL14] and a Type C analog by Sulzgruber and Thiel [ST14]. Rational Dyck paths also are intimately entwined in the study of rational parking functions and MacDonal polynomials, with

Key words and phrases. Dyck path, rational Dyck path, lattice path, core partition, zeta map, eta map, sweep map, lasers, conjugate-area map, area statistic, dinv statistic, exceedence, regression decision tree.

The first author was supported by the government of Canada through a Banting Postdoctoral Fellowship. He was also supported by a York University research grant. The second author was supported by a postdoctoral fellowship with York University and the Fields Institute, with additional support from NSERC. The third author gratefully acknowledges support from PSC-CUNY Research Awards TRADA-44-168 and TRADA-45-60.

recent work by Gorsky, Mazin, and Vazirani [GMV14] and when a and b are not relatively prime by Bergeron, Garsia, Levin, and Xin [BGLX14].

Our goal is to explore the following conjecture:

Conjecture 1.1. Let a and b be relatively prime positive integers. The *zeta map* $\zeta : \mathfrak{D}_{a,b} \rightarrow \mathfrak{D}_{a,b}$ is a bijection.

Our perspective is that there are in fact two maps, the zeta map and the eta map, which jointly contain enough information to recover the original path. In Section 6.1, we provide a straightforward algorithm for recovering P from the combined data of $Q = \zeta(P)$ and $R = \eta(P)$. What we find interesting is that the information contained solely in $\zeta(P)$ does not seem to be enough to reconstruct P directly. Our argument does not give an explicit construction of $\zeta^{-1}(Q)$, nor do we construct a bounce path.

Our eta map is based on a natural notion of conjugation on rational Dyck paths explored in Section 4 that arises from Anderson’s bijection [And02] between (a, b) -Dyck paths and simultaneous (a, b) -core partitions, which in turn are related to many more combinatorial interpretations. (See [AHJ14] for additional background.) Our map η is defined by $\eta(P) = \zeta(P^c)$, and in most cases $\zeta(P) \neq \eta(P)$. Section 5 is devoted to presenting the algorithms for calculating the zeta map and the eta map in multiple fashions. In particular, we present two new methods involving lasers and interval intersections.

Meanwhile, ζ and η combine to induce a new *area-preserving* involution χ on the set of Dyck paths defined in Section 6.2 by

$$\chi(Q) := \eta(\zeta^{-1}(Q)) = \zeta(\zeta^{-1}(Q)^c).$$

In Section 7, we prove that in the classical Catalan case, this *conjugate-area map* χ is the map that reverses the Dyck path. Applying our inverse algorithm presents a new construction of the inverse of the zeta map on a Dyck path. However, we have no explicit description of $\chi(Q)$ from Q in the general (a, b) -case. Indeed, a concrete construction of $\chi(Q)$ from Q could be used to construct an explicit inverse for the zeta map.

In Section 8, we show that when a rational Dyck path Q visits the lattice point having level equal to 1, $\zeta^{-1}(Q)$ has a nice decomposition as does its image under the conjugate-area map χ . These observations allows us to explicitly find χ (and therefore ζ^{-1}) of any path that has valleys exactly on levels equal to $\{1, \dots, k\}$ for $k < a$ in Theorem 8.3. We have also constructed $\chi(Q)$ and $\zeta^{-1}(Q)$ for paths that bound left-adjusted or up-adjusted partitions in Proposition 6.11.

Section 9 presents two promising avenues for proving Conjecture 1.1. Section 9.1 discusses a key permutation $\gamma(P)$ that serves to fully encode P , $\zeta(P)$, and $\eta(P)$ by way of its excedences. Section 9.2 investigates the poset of rational Dyck paths ordered by when one path is weakly below the other, motivating a new statistic $\delta(P)$ that appears to be fruitful for recursively computing ζ^{-1} from evidence gathered by computer learning algorithms. Indeed, in the remainder of Section 9, we use $\delta(P)$ to construct the initial part of a rational bounce path and to give a new algorithm that computes ζ^{-1} for $(a, am + 1)$ -Dyck paths. This provides an alternate proof of the bijectivity of the zeta map on $(a, am + 1)$ -Dyck paths to that of Loehr in [Loe05].

One of our primary motivations was the study of conjectured statistics for the q, t -enumeration of (a, b) -Dyck paths. Section 2 sets the stage by introducing key combinatorial concepts and statistics associated to (a, b) -Dyck paths. In Section 3 we investigate the *skew length* statistic $sl(P)$, originally defined in the context of (a, b) -cores in [AHJ14]. The original definition of skew length seems to depend on the ordering of a and b ; we show that skew length is in fact independent of this choice. The main tools we develop involve a row length filling of the boxes under the (a, b) -Dyck path P and above the main diagonal, along with the idea of skew inversions and flip skew inversions. Section 4 shows that *skew length* is preserved under conjugation.

Enjoy reading and we’d love to hear your feedback!

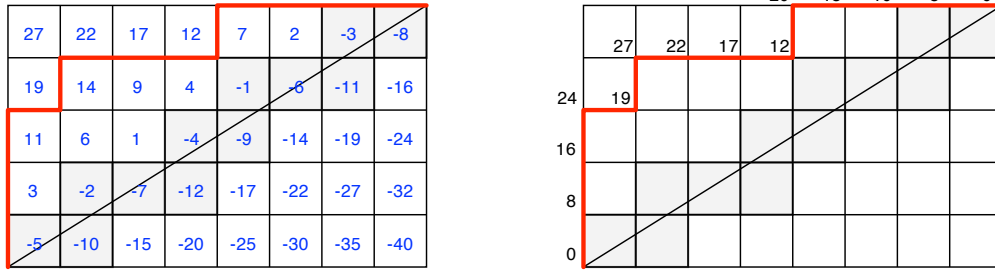


FIGURE 1. (Left) A lattice path P when $a = 5$ and $b = 8$. The hook filling is given by the numbers in the center of the boxes. The boxes above the path show that the partition bounded by P is $(4, 1)$.

(Right) The levels of the lattice points along the path.

2. BACKGROUND AND NOTATION

Definition 2.1. An (a, b) -lattice path P is a lattice path in \mathbb{Z}^2 consisting of north and east steps starting from the origin and ending at the point (b, a) .

We call P an (a, b) -Dyck path if P remains (weakly) above the diagonal line connecting the origin to (b, a) . Equivalently, the lattice points (x, y) along P satisfy $ax \leq by$. We draw (a, b) -Dyck paths in an $a \times b$ grid, where the lower left corner is the origin.

We denote the full collection of (a, b) -Dyck paths by $\mathfrak{D}_{a,b}$, or simply \mathfrak{D} if there is no confusion about the values of a and b .

We use the English notation for Young diagrams, drawing the largest row at the top. The *hook length* of a box B in the Young diagram of a partition is the number of boxes in the *hook* of boxes directly below or directly to the right of B , including the box B itself. An a -core partition (or simply a -core) is a partition for which its Young diagram has no boxes with hook length equal to a . Similarly, a *simultaneous* (a, b) -core partition (or (a, b) -core for short) has no hooks equal to a or b .

Anderson proved that when a and b are relatively prime there are finitely many (a, b) -cores [And02] by finding a bijection with the set of (a, b) -Dyck paths; these are counted by the formula

$$\frac{1}{a+b} \binom{a+b}{a}.$$

This formula seems to have been discovered at various times; the earliest reference we know of is [DM47] in 1947. In 1954, Bizley considered the general case of rectangular Dyck paths of which this formula is a special case [Biz54].

Bizley's counting method starts from the full set of lattice paths from $(0, 0)$ to (b, a) , and considers the orbit of the cyclic group C_{a+b} acting by *cyclic shifts* on paths. In the case where a and b are relatively prime, there is a unique Dyck path in each such orbit.

Example 2.2. Let N and E represent a north step and an east step, respectively. Throughout this paper, we will use as our running example the $(5, 8)$ -Dyck path

$$P = NNNENEENEENE,$$

shown in Figure 1.

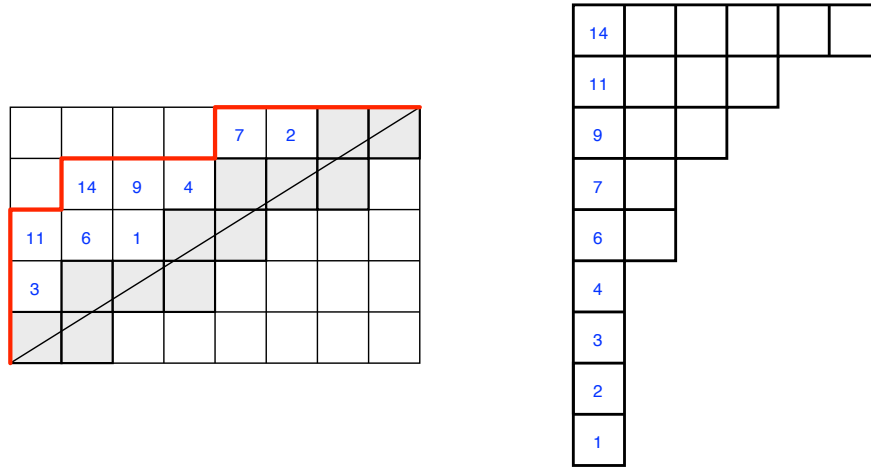


FIGURE 2. Anderson’s bijection gives a correspondence between (a, b) -Dyck paths and (a, b) -core partitions. Corresponding to $P = NNNENEEENE$ is the $(5, 8)$ -core $(6, 4, 3, 2, 2, 1, 1, 1, 1)$.

2.1. Dictionary of notation.

We keep track of numerous bits of data associated to an (a, b) -Dyck path P .

(1) General constructions:

- The *hook filling* of the boxes in the square lattice is obtained by filling the box with lower-right lattice point $(b, 0)$ with the number $-ab$ and increasing by a for every one box west and increasing by b for every one box north. A box is above the main diagonal if and only if the corresponding hook is positive. (See Figure 1.)
- The *positive hooks* of P are the numbers in the hook filling below the path but greater than zero. (Elsewhere these have been called *beta numbers* or *bead numbers*.)
- We denote by $\mathfrak{c}(P)$ the (a, b) -core corresponding to P under Anderson’s bijection. The hook lengths of the boxes in the first column of $\mathfrak{c}(P)$, its *leading hooks*, are precisely the positive hooks of P . An example of Anderson’s bijection is illustrated in Figure 2.
- The *row length filling* of P are numbers placed in the boxes under P . They correspond to the number of boxes in the row of $\mathfrak{c}(P)$ with the given hook. This will be developed in Section 3.2. (See Figure 5.)
- The *partition bounded by P* is the partition whose Young diagram is the collection of boxes above the path P .

(2) Combinatorial statistics:

- The *area* of P , denoted $\text{area}(P)$ is the number of positive hooks of P . Equivalently, this is the number of rows in $\mathfrak{c}(P)$.
- The *rank* of P , denoted $\text{rk}(P)$ is the number of rows in the partition bounded by P .
- The *skew length* of P , denoted $\text{sl}(P)$ is a statistic that we discuss in detail in Section 3.

(3) Sets and sequences of numbers associated to P :

- The *levels* of P are labels associated to the lattice points of P defined by Armstrong, Loehr, and Warrington in [ALW14a, ALW14b]. Assign level 0 to $(0, 0)$ and label the other lattice points of P by adding b after each north step and subtracting a after each east step. Equivalently, this is the value of the hook filling in the box to the northwest of the lattice point. Note that the label of the northeast-most lattice point (b, a) is once again $0 + a \cdot b - a \cdot b = 0$.
- The path P has two reading words obtained by reading the levels in order. The *reading word* of P , denoted $L(P)$ (for ‘levels’), is obtained by reading the levels that occur along

the path from southwest to northeast, excluding the final 0. (One can imagine assigning to each north and east step of the path the level of the step's initial lattice point.)

The *reverse reading word*, denoted $M(P)$, is obtained by reading from northeast to southwest, excluding the final 0. (One can imagine P as a path from (b, a) to $(0, 0)$ consisting of west and south steps, once again assigning to each step the level of its initial lattice point.)

Reading along P in Figure 1 shows that

$$L(P) = (0, 8, 16, 24, 19, 27, 22, 17, 12, 20, 15, 10, 5)$$

and

$$M(P) = (0, 5, 10, 15, 20, 12, 17, 22, 27, 19, 24, 16, 8).$$

When a and b are relatively prime, no value occurs more than once in $L(P)$ or $M(P)$.

- The set of levels of P is partitioned into the set of *north levels* $N(P)$ and *east levels* $E(P)$, where when reading from southwest to northeast, levels of lattice points starting north steps of P are in $N(P)$ and levels of lattice points starting east steps of P are in $E(P)$. We order these levels in decreasing order. In our running example, the north levels of P are

$$N(P) = \{19, 16, 12, 8, 0\},$$

and the east levels of P are

$$E(P) = \{27, 24, 22, 20, 17, 15, 10, 5\}.$$

- (4) **Permutations associated to P :** Throughout the paper we use square brackets to write permutations in one-line notation, and round parentheses for permutations in cycle notation.

- The *reading permutation* of P is a permutation σ in S_{a+b} that encodes the relative order of the levels recorded in $L(P)$. The *reverse reading permutation* of P , denoted $\tau(P)$, encodes the relative order of the values in $M(P)$. In our running example, the one-line notation for $\sigma(P)$ and $\tau(P)$ are

$$\sigma(P) = [1, 3, 7, 12, 9, 13, 11, 8, 5, 10, 6, 4, 2]$$

and

$$\tau(P) = [1, 2, 4, 6, 10, 5, 8, 11, 13, 9, 12, 7, 3].$$

- Let $\gamma(P)$ be the permutation in S_{a+b} that when written in cycle notation is equivalent to $\sigma(P)$ written in one-line notation. In our running example P we have

$$\begin{aligned} \gamma(P) &= (1, 3, 7, 12, 9, 13, 11, 8, 5, 10, 6, 4, 2) \\ &= [3, 1, 7, 2, 10, 4, 12, 5, 13, 6, 8, 9, 11]. \end{aligned}$$

Remark 2.3. The path P can be recovered knowing only $\sigma(P)$ (or $\tau(P)$ or $\gamma(P)$). The east steps of P correspond exactly to the right (cyclic) descents[†] of σ ; whereas, the north steps of P correspond to the right (cyclic) ascents of σ .

3. SKEW LENGTH

In [AHJ14] the *skew length* statistic is proposed as a q -statistic for (a, b) -Dyck paths and a related construction is investigated in [ALW14a, Section 4]. In this section, we present the original definition of skew length on cores and two equivalent interpretations on (a, b) -Dyck paths using length fillings and skew inversions. We show that these interpretations are indeed equivalent to the original definition and, as a consequence, we prove that skew length is independent of the

[†]A descent of a permutation occurs when $\sigma(i) > \sigma(i+1)$. A cyclic descent is defined in the same way, but considering the indices modulo $a+b$, allowing a descent in the last position of σ .

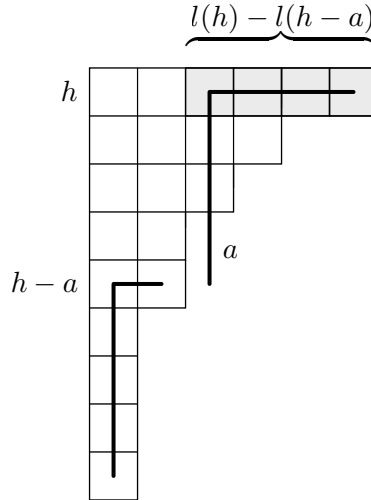


FIGURE 3. The number of a -boundary boxes in the row of κ corresponding to a leading hook h is $l(h) - l(h - a)$.

ordering of a and b . Further interpretations of skew length are presented in terms of the zeta map in Section 5.

3.1. Skew length on cores and polynomial motivation.

We begin with an observation on ordinary core partitions before discussing simultaneous core partitions.

Definition 3.1 ([AHJ14, Definition 2.7]). Let κ be an a -core partition. Consider the hook lengths of the boxes in the first column of κ . Find the largest hook length of each residue modulo a . The a -rows of κ are the rows of κ corresponding to these hook lengths. The a -boundary of κ consists of all boxes in its Young diagram with hook length less than a .

Proposition 3.2. *Let κ be an a -core partition. The number of boxes in the a -rows of κ equals the number of boxes in the a -boundary of κ .*

Proof. Let $l(h)$ be the number of boxes in the row of κ with leading hook h .

We first observe that if $h > a$ is a leading hook of κ , then $h - a$ is also a leading hook of κ . For this, decompose h into two hooks of lengths $h - a$ and a as illustrated in Figure 3, such that the boxes in the row with leading hook h that are intersected by the hook a are exactly the boxes in the a -boundary in that row. This guarantees that the right-end box of the hook $h - a$ is in κ , and therefore that $h - a$ is also a leading hook.

Now, the number of a -boundary boxes in the row of κ corresponding to h is $l(h) - l(h - a)$. Summing over all rows gives the number of a -boundary boxes; telescoping over residues modulo a gives the number of boxes in the a -rows of κ . \square

Corollary 3.3. *The number of boxes in the a -rows of κ equals the number of boxes in the a -rows of κ^c*

Remark 3.4. For readers familiar with the abacus diagram interpretation, hook lengths correspond to beads on the abacus; the a -rows correspond to the largest bead on each runner of the a -abacus. Proposition 3.2 gives a way to count the number of boxes in the a -boundary of an a -core by adding the number of gaps that appear on the abacus before each of these largest beads.

Definition 3.5 ([AHJ14, Definition 2.7]). Let κ be an (a, b) -core partition. The *skew length* of κ , denoted $sl(\kappa)$, is the number of boxes simultaneously located in the a -rows and the b -boundary of κ .

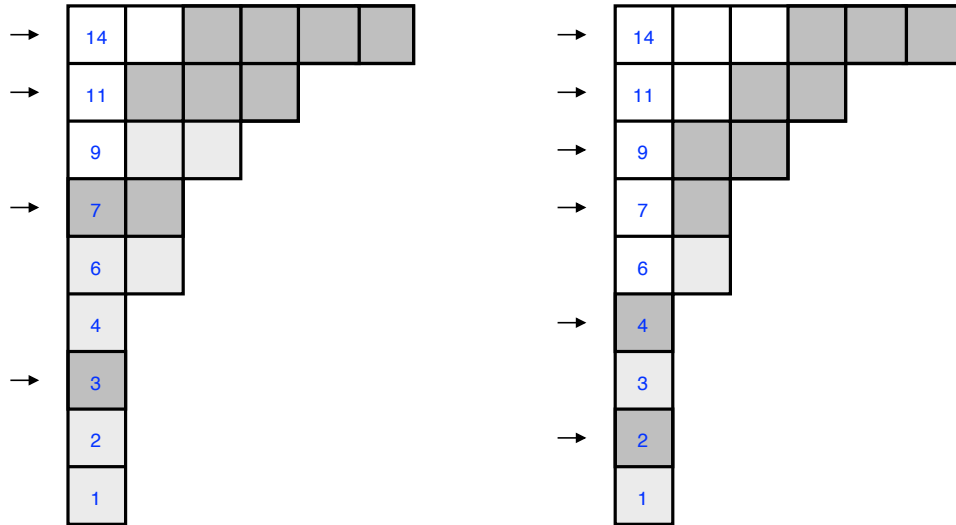


FIGURE 4. (Left) The 8-boundary boxes of our favorite $(5, 8)$ -core κ are shaded; those in the 5-rows of κ are darker. (Right) The 5-boundary boxes of κ are shaded; those in the 8-rows of κ are darker. Surprisingly, the number of darkly shaded boxes on the left $4 + 3 + 2 + 1 = 10$ is equal to the number of darkly shaded boxes on the right $3 + 2 + 2 + 1 + 1 + 1 = 10$. (See Corollary 3.18.)

Example 3.6. The core partition shown in Figure 4 is the $(5, 8)$ -core $\kappa = \mathfrak{c}(P)$ corresponding to the path P in our running example from Figures 1 and 2.

On the left, the 5-rows of κ are the rows with leading hook lengths 14, 11, 7, and 3. The darkly shaded boxes are those boxes in the 5-rows with hook length less than 8. The skew length is equal to $4 + 3 + 2 + 1 = 10$.

On the right, we compute of the skew length of κ when considered as an $(8, 5)$ -core. The 8-rows of κ are the rows with leading hook lengths 14, 11, 9, 7, 4, and 2. The shaded boxes are those boxes in the 8-rows with hook length less than 5. The skew length is equal to $3 + 2 + 2 + 1 + 1 + 1 = 10$.

We will see in Corollary 3.18 that it is not a coincidence that these two numbers are the same.

The number of boxes in the 8-boundary (shaded boxes, left) equals the number of boxes in the 8-rows (marked rows, right) and the number of boxes in the 5-boundary (shaded boxes, right) equals the number of boxes in the 5-rows (marked rows, left), as proved in general in Proposition 3.2.

The skew length statistic was found by Armstrong; he conjectures it as a key statistic involved in the q - and q, t -enumeration of (a, b) -cores (or (a, b) -Dyck paths). Recall that the rank $\text{rk}(\kappa)$ of an (a, b) -core κ is the number of rows in its corresponding Young diagram.

Conjecture 3.7. [AHJ14, Conjecture 2.8] Let a and b relatively prime positive integers. The expression

$$f_{a,b}(q) = \frac{1}{[a+b]_q} \begin{bmatrix} a+b \\ a \end{bmatrix}_q$$

is equal to the polynomial

$$g_{a,b}(q) = \sum_{\kappa} q^{\text{sl}(\kappa) + \text{rk}(\kappa)},$$

where the sum is over all (a, b) -cores κ .

Haiman [Hai94, Proposition 2.5.2] proved that $f_{a,b}(q)$ is a polynomial if and only if a and b are relatively prime, but there is no simple proof that $f_{a,b}(q)$ has non-negative coefficients. ([GG12,

Section 1.12] provides a proof involving representation theory of rational Cherednik algebras.) Conjecture 3.7 would provide such a proof.

Proposition 3.8. [Hai94, GG12] *The expression*

$$f_{a,b}(q) = \frac{1}{[a+b]_q} \begin{bmatrix} a+b \\ a \end{bmatrix}_q$$

is a polynomial if and only if $\gcd(a,b) = 1$. Furthermore, when a and b are relatively prime, the resulting polynomial has integer coefficients.

Define the *co-skew length* of an (a,b) -core κ as

$$\text{sl}'(\kappa) := \frac{(a-1)(b-1)}{2} - \text{sl}(\kappa).$$

Armstrong conjectures that rank and co-skew length give a q, t -enumeration of the (a,b) -cores, subject to the following symmetry:

Conjecture 3.9. [AHJ14, Conjecture 2.9] The following q, t -polynomials are equal:

$$\sum q^{\text{rk}(\kappa)} t^{\text{sl}'(\kappa)} = \sum q^{\text{sl}'(\kappa)} t^{\text{rk}(\kappa)}$$

where the sum is over all (a,b) -cores κ .

These q, t -polynomials are called the *rational q, t -Catalan numbers*.

Remark 3.10. As an aside, we have observed that $f_{a,b}(q)$ is particularly resilient to deformation. In [SS10], a Fibonacci ‘deformation’ of the binomial coefficients is introduced, alongside combinatorial interpretations thereof. In this scheme, each integer k is replaced by a Fibonacci number F_k , with the Fibonacci numbers initialized as $F_0 = 0$ and $F_1 = 1$. The resulting ‘Fibonomial’ coefficients

$$\begin{Bmatrix} F_{a+b} \\ F_a \end{Bmatrix} = \frac{F_{a+b} F_{a+b-1} \cdots F_1}{F_a F_{a-1} \cdots F_1 F_b F_{b-1} \cdots F_1}$$

are shown by Sagan and Savage to be integers. Define the (a,b) -*Fibolan* as:

$$F_{a,b} = \frac{1}{F_{a+b}} \begin{Bmatrix} F_{a+b} \\ F_a \end{Bmatrix}.$$

We can also apply a double-deformation, and speak of q -Fibonacci numbers. Here we replace each Fibonacci number F_k with the q -polynomial $[F_k]_q = 1 + q + \cdots + q^{F_k-1}$. Then we may define the q - (a,b) -Fibolans as:

$$F_{a,b}(q) = \frac{1}{[F_{a+b}]_q} \begin{Bmatrix} F_{a+b} \\ F_a \end{Bmatrix}_q.$$

Somewhat amazingly, the q - (a,b) -Fibolans are still polynomials in q . The Fibonacci numbers admit a Euclidean algorithm; in particular, we have that $\gcd(F_a, F_b) = F_{\gcd(a,b)}$. The proof of polynomiality in Proposition 3.8 can then be adapted exactly to the study of the q - (a,b) -Fibolans. In this case, the proof gives us that the q - (a,b) -Fibolan is a polynomial if and only if $\gcd(F_a, F_b) = F_{\gcd(a,b)} = 1$, which occurs if and only if $\gcd(a,b) = 1$ or 2 . It would be interesting to have a combinatorial interpretation of these q -deformed (a,b) -Fibolan numbers. This connection will be explored in more detail in [ABCL15].

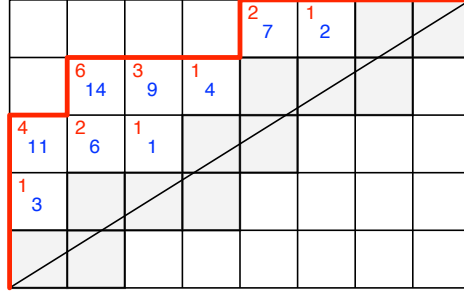


FIGURE 5. The row length filling of boxes below the path P is given in red in the upper left corner. The values correspond to the length of the rows of $\mathfrak{c}(P)$ in Figure 2.

3.2. Skew length on Dyck paths via the row length filling.

We now provide a new method to calculate the skew length of an (a, b) -Dyck path P which uses a *row length filling* of the boxes below P . Our method coincides with the skew length statistic proposed by Armstrong for (a, b) -cores. As a consequence, we show that skew length of an (a, b) -core is independent of the ordering of a and b .

We provide two equivalent definitions of the *row length filling*.

Definition 3.11. Let P be an (a, b) -Dyck path. The *row length filling* of P is an assignment of numbers to each box below the path P .

For a box B with positive hook filling h , define the row length of B to be the length of the row in $\mathfrak{c}(P)$ with leading hook h . Alternatively, define the row length of B to be $h - p_h$, where p_h is the number of positive entries in the hook filling strictly less than h .

For a box B with non-positive hook filling h , define the row length of B to be zero.

For any hook h in the hook filling of P , we denote by $l(h)$ the corresponding value of the row length filling of P .

Figure 5 shows in red in the upper left corner the row length of the boxes corresponding to the positive hooks of P .

Lemma 3.12. *The two definitions of row length filling in Definition 3.11 are equivalent.*

Proof. When ordered in increasing order, the entries in the hook filling of P correspond to the hook lengths of the boxes in the first column of $\mathfrak{c}(P)$ from shortest to longest. Suppose the first box of the i th shortest row has hook length h . Then the length of the i th shortest row is $h - (i - 1)$, which is exactly the corresponding entry in the row length filling. \square

Remark 3.13. For readers familiar with the abacus diagram interpretation, the row length filling associates to each bead on the abacus the number of gaps that appear on the abacus before it.

The row length filling is very useful for reading off common core statistics from the Dyck path. For example, we can immediately see that:

Corollary 3.14. *The sum of the entries of the row length filling of P is equal to the number of boxes of the core $\mathfrak{c}(P)$.*

Furthermore, because the a -rows of $\mathfrak{c}(P)$ correspond to the westmost boxes under P and the b -rows of $\mathfrak{c}(P)$ correspond to the northmost boxes under P , the number of boxes in $\mathfrak{c}(P)$ with hook length less than a or less than b can be determined from the row length filling as a direct consequence of Proposition 3.2.

Corollary 3.15. *The number of boxes in the a -boundary of an (a, b) -core $\mathfrak{c}(P)$ is equal to the sum of the row length fillings of the westmost boxes under P . Likewise, the number of boxes in the b -boundary of $\mathfrak{c}(P)$ is equal to the sum of the row length fillings of the northmost boxes under P .*

In the same vein, the skew length of P can also be easily computed, as follows:

Theorem 3.16. *The skew length of an (a, b) -core $\mathfrak{c}(P)$ may be computed from the length filling of P by adding all lengths at outer corners and subtracting all lengths at inner corners.*

Proof. By the argument in the proof of Proposition 3.2, we see that when h is a positive hook of an (a, b) -Dyck path P (so that $h - a$ is the hook of the box directly east of the box with hook h and $h - b$ is the hook of the box directly south of the box with hook h), then

- (i) The number of a -boundary boxes in the row of $\mathfrak{c}(P)$ corresponding to h is $l(h) - l(h - a)$.
- (ii) The number of b -boundary boxes in the row of $\mathfrak{c}(P)$ corresponding to h is $l(h) - l(h - b)$.

By restricting to the a -rows or b -rows, we see that the skew length of $\mathfrak{c}(P)$ is given by:

$$(3.1) \quad \sum l(h) - l(h - b),$$

where the sum is over all westmost boxes under P , or alternatively the skew length of $\mathfrak{c}(P)$ is given by:

$$(3.2) \quad \sum l(h) - l(h - a),$$

where the sum is over all northmost boxes under P . When one westmost box under P is directly north of another, Formula (3.1) telescopes. After cancelling terms, we are left with the lengths at outer corners of P minus the lengths at inner corners of P . An equivalent argument can be made from Formula (3.2). \square

Example 3.17. In Figure 5, we see that the sum of the row length fillings is 21, which is the number of boxes of $\mathfrak{c}(P)$. Adding the row lengths of the westmost boxes under P gives $2 + 6 + 4 + 1 + 0 = 13$ boxes in the 5-boundary of $\mathfrak{c}(P)$, while adding the row lengths of the northmost boxes under P gives $4 + 6 + 3 + 1 + 2 + 1 + 0 + 0 = 17$ boxes in the 8-boundary of $\mathfrak{c}(P)$, as expected from Figure 4. Our path P has three outer corners with row lengths 2, 6, and 4 and two inner corners with row lengths 2 and 0. The skew length of our path is then

$$\text{sl}(P) = (2 + 6 + 4) - (2 + 0) = 10.$$

When computing skew length directly from the core, it is not obvious that the number of boxes in a -rows and the b -boundary should be equal to the number of boxes in b -rows and the a -boundary (see Figure 4). But the method of computing the skew length given by Theorem 3.16 is independent of the ordering of a and b : Switching a and b flips the rectangle to a $b \times a$ rectangle in which outer corners are still outer corners, inner corners are still inner corners, and the hook filling and row length filling are otherwise unaffected.

Corollary 3.18. *The skew length of an (a, b) -core κ is independent of the ordering of a and b .*

3.3. Skew length via skew inversions.

This section presents another interpretation of the skew length of an (a, b) -Dyck path P in terms of the number of its *skew inversions* or the number of its *flip skew inversions*.

Recall that the north levels of P are the levels $\mathbf{N}(P) = \{n_1, \dots, n_a\}$ of the initial lattice points of the north steps in the path, and that the east levels of P are the levels $\mathbf{E}(P) = \{e_1, \dots, e_b\}$ of the initial lattice points of the east steps.

Definition 3.19. A *skew inversion* of P is a pair of indices (i, j) such that $n_i > e_j$. A *flip skew inversion* of P is a pair of indices (i, j) with $n_i + b < e_j - a$.

Theorem 3.20. *Let P be an (a, b) -Dyck path. The skew length of P equals the number of skew inversions of P , which is equal to the number of flip skew inversions of P .*

The key to the proof of Theorem 3.20 is recognizing the relationship between westmost boxes under P and north levels in $\mathbf{N}(P)$ and the relationship between northmost boxes under P and east levels in $\mathbf{E}(P)$.

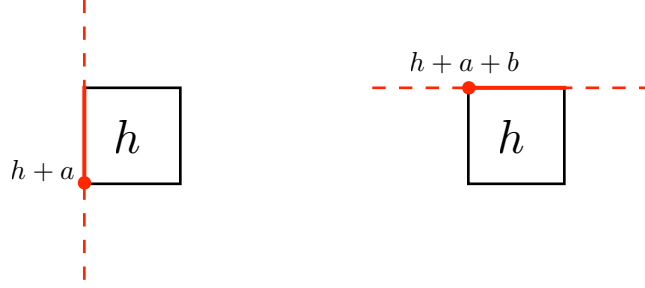


FIGURE 6. When h is the hook filling of a westmost box under P , the associated north level is $n_h = h + a$. When h is the hook filling of a northmost box under P , the associated east level is $e_h = h + a + b$.

Remark 3.21. Figure 6 shows that when h is the hook filling of a westmost box under P , then the associated north level n_h (corresponding to the lattice point at its southwest corner) is $h + a$. When h is the hook filling of a northmost box under P , then the associated east level e_h (corresponding to the lattice point at its northwest corner) is $h + a + b$.

Lemma 3.22. *Let h be the hook filling of a westmost box under an (a, b) -Dyck path P . The length difference $l(h) - l(h - b)$ is equal to the number of skew inversions involving the associated north level n_h , which equals the number of b -boundary boxes in the a -row corresponding to h .*

Proof. Recall that $l(h) = h - p_h$, where p_h is the number of positive hooks in the hook filling of P less than h . Then:

$$\begin{aligned} l(h) - l(h - b) &= h - p_h - (h - b) + p_{h-b} \\ &= b - (p_h - p_{h-b}) \\ &= b - \#\{g \mid h - b \leq g < h\}. \end{aligned}$$

Each box with hook filling g satisfying the inequalities $h - b \leq g < h$ is in a distinct column of the diagram of P . If two were in the same column, then the difference of their hooks would be a multiple of b , so that both could not satisfy the inequality. As a result, we may add a multiple of b to each g satisfying the inequalities to obtain a unique northmost box under P with hook filling \bar{g} satisfying $h - b \leq \bar{g}$. Conversely, for every northmost box under P with hook filling \bar{g} satisfying this inequality there is a unique box with hook filling g in the same column satisfying $h - b \leq g < h$. Therefore,

$$\begin{aligned} l(h) - l(h - b) &= b - \#\{\bar{g} \mid h - b \leq \bar{g}\} \\ &= \#\{\bar{g} \mid h - b > \bar{g}\}. \end{aligned}$$

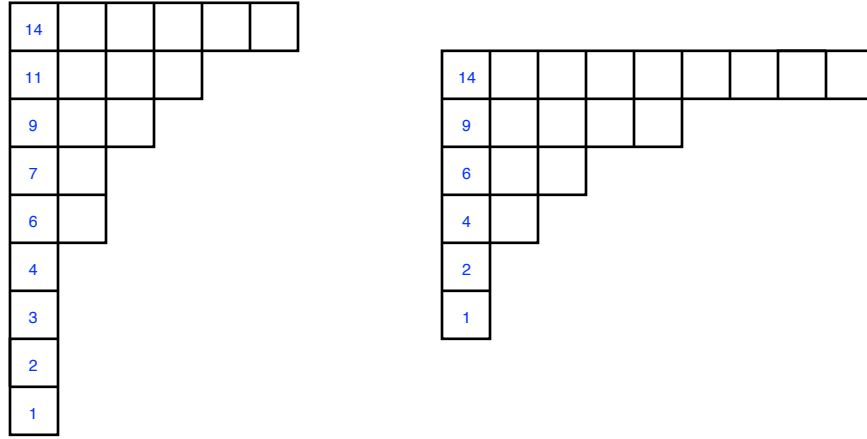
By Remark 3.21, this is equivalent to $l(h) - l(h - b) = \#\{e_j \mid n_h > e_j\}$, as desired. The last clause of the statement of the lemma is given in the proof of Theorem 3.16. \square

Similar arguments prove the following.

Lemma 3.23. *Let h be the hook filling of a northmost box under an (a, b) -Dyck path P . The length difference $l(h) - l(h - a)$ is equal to the number of flip skew inversions involving the associated east level e_h , which equals the number of a -boundary boxes in the b -row corresponding to h .*

Theorem 3.20 now follows directly from Definition 3.5 by summing over all westmost boxes in Lemma 3.22 and all northmost boxes in Lemma 3.23.

Example 3.24. In our running example, the north levels are $\mathbf{N} = \{19, 16, 12, 8, 0\}$ and the east levels are $\mathbf{E} = \{27, 24, 22, 20, 17, 15, 10, 5\}$. There are 10 skew inversions because there are 4 east

FIGURE 7. The conjugate map on (a, b) -cores.

levels less than $n_1 = 19$, 3 east levels less than $n_2 = 16$, 2 east levels less than $n_3 = 12$, 1 east levels less than $n_4 = 8$, and 0 east levels less than $n_5 = 0$. The total number of skew inversions is then $4 + 3 + 2 + 1 + 0 = 10$. These numbers correspond to the number of b -boundary boxes in the a -rows of the core $\mathfrak{c}(P)$ in Figure 4.

To calculate the flip skew inversions, consider the sets $\mathbf{N} + b = \{27, 24, 20, 16, 8\}$ and $\mathbf{E} - a = \{22, 19, 17, 15, 12, 10, 5, 0\}$. There are 10 flip skew inversions because there are 3 elements of the form $n_i + b$ less than $e_1 - a = 22$, there are 2 less than $e_2 - a = 19$, 2 less than $e_3 - a = 17$, 1 less than $e_4 - a = 15$, 1 less than $e_5 - a = 12$, 1 less than $e_6 - a = 10$, 0 less than $e_7 - a = 5$, and 0 less than $e_8 - a = 0$. The total number of flip skew inversions is then $3 + 2 + 2 + 1 + 1 + 1 + 0 + 0 = 10$. These numbers correspond to the number of a -boundary boxes in the b -rows of the core $\mathfrak{c}(P)$.

Remark 3.25. Skew inversions in an (a, b) -Dyck path arise from pairs of north levels and east levels where $n_i > e_j$. Note that $n_i + b$ is the level of the terminal lattice point of the corresponding north step (instead of initial lattice point), while $e_j - a$ is the level of the terminal lattice point of the corresponding east step. So flip skew inversions are best understood by a reverse reading of P as a sequence of west and south steps, counting the pairs where the south level is less than the west level. Alternatively, flip skew inversions of P correspond to skew inversions of P when P is reflected (flipped) to be a (b, a) -Dyck path.

4. THE CONJUGATE MAP

For any partition κ , its conjugate partition κ^c is obtained by reflecting along its main diagonal. (See Figure 7.) Since hook lengths are preserved under this reflection, when κ is an (a, b) -core, so is κ^c . When a and b are relatively prime, there is a natural conjugate map on (a, b) -Dyck paths P . Apply cyclic shifts to the path P until we encounter a path strictly *below* the diagonal, the conjugate path P^c is the result of rotating this path 180° . (See Figure 8.) The first main result of this section (Theorem 4.1) shows that these conjugations are equivalent under Anderson's bijection, and the second (Theorem 4.5) shows that conjugation preserves skew length. These two results were simultaneously found in independent work by Xin in [Xin15b].

Theorem 4.1. *Conjugation on (a, b) -cores coincides with conjugation on (a, b) -Dyck paths via Anderson's bijection:*

$$\mathfrak{c}(P)^c = \mathfrak{c}(P^c).$$

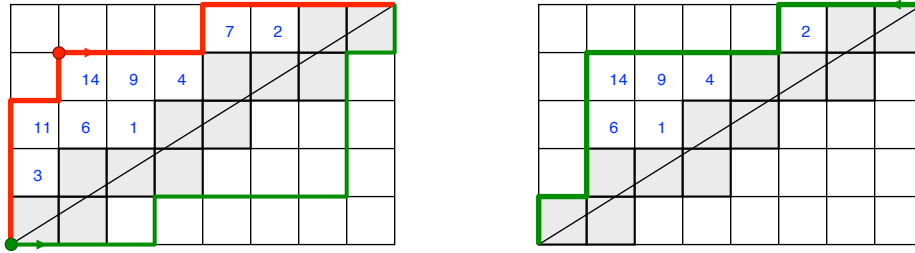


FIGURE 8. The conjugate map on (a, b) -Dyck paths.

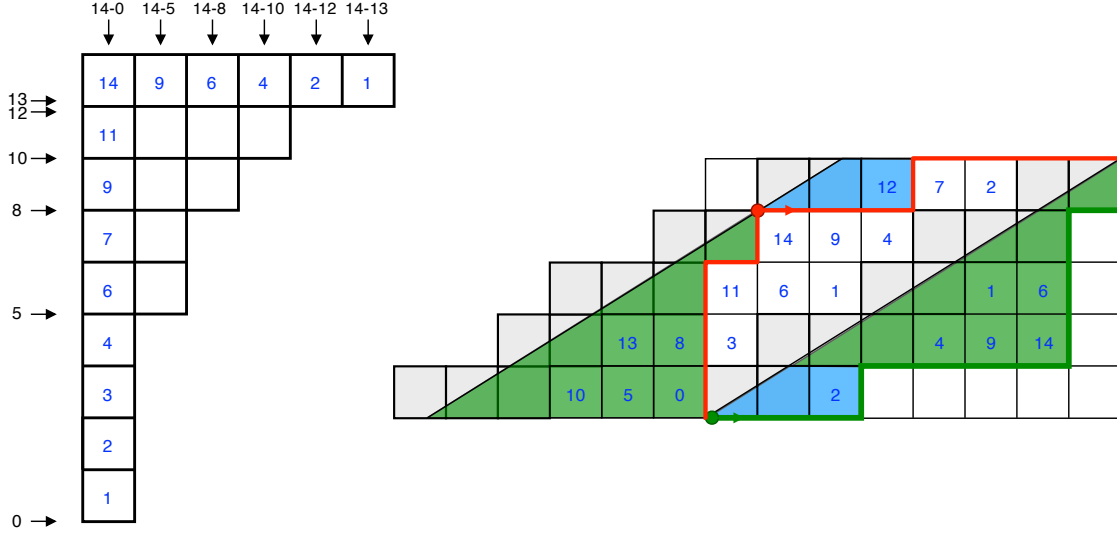


FIGURE 9. Illustration of the proof of Lemmas 4.2 and 4.3

This follows directly by showing the equivalence between the leading hooks of $\mathfrak{c}(P)^c$ and the positive hooks of P^c . A result of Olsson gives the leading hooks of $\mathfrak{c}(P)^c$; we include a proof for completeness.

Lemma 4.2. [Ols93, Lemma 2.2] *Let κ be any partition with leading hooks given by the set H , with $m = \max(H)$. The conjugate partition κ^c has leading hooks given by $\{m - n : n \in \{0, 1, \dots, m\} \setminus H\}$.*

Proof. Let κ be any partition with leading hooks (hooks in the first column) given by the set H , with $m = \max(H)$. The leading hooks of its conjugate partition are the hooks in the top row of κ . This partition has one column for each number n in the set $\{0, 1, \dots, m\} \setminus H$. The hook of the upper box in the column corresponding to n is equal to $m - n$ as illustrated in Figure 9. \square

Lemma 4.3. *Let P be an (a, b) -Dyck path with positive hooks given by H , with $m = \max(H)$. The conjugate path P^c has positive hooks given by $\{m - n : n \in \{0, 1, \dots, m\} \setminus H\}$.*

Proof. Let P be an (a, b) -Dyck path with positive hook set given by H and where $m = \max(H)$. Fill all the boxes on the left of the path with the hooks that are less than m . Hooks appearing in the same row are equivalent mod a . Furthermore, the rows contain all the residues $0, 1, \dots, a - 1$ modulo a because a and b are relatively prime and, as a consequence, the filled hooks contain all the numbers from 0 to m .

Draw a diagonal parallel to the main diagonal passing through the upper left corner of the box below P with the largest hook m . Consider the area A below this diagonal directly on the left of

P as illustrated in Figure 9. The boxes in A are exactly the boxes on the left of the path with hook length n less than m . Applying cyclic shifts to P to obtain a path below the main diagonal transforms the area A to the area between the main diagonal and the shifted path. Since this transformation maps the box with hook length m to the box with hook length 0 (when rotated 180 degrees), the hook length n gets transformed to the hook length $m - n$. \square

Example 4.4. In both Figure 7 and Figure 8, the set of hooks on the left is $H = \{1, 2, 3, 4, 6, 7, 9, 11, 14\}$, with $m = 14$. The set $\{0, 1, \dots, m\} \setminus H = \{0, 5, 8, 10, 12, 13\}$, and subtracting these numbers from 14 we get that the leading and positive hooks of the conjugate are $\{14, 9, 6, 4, 2, 1\}$ as desired.

Theorem 4.5. *The skew length of P is equal to the skew length of P^c .*

Proof. Let $n_i < e_j$ be a skew inversion for the path P , with largest level m . The north and east steps of the conjugate path are in correspondence with the north and east steps in the original path, respectively. The corresponding north and east levels are given by $n'_i = m - n_i - b$ and $e'_j = m - e_j + a$. A simple calculation shows that these satisfy $n'_i + b < e'_j - a$, giving a flip skew inversion for P^c . Thus, there is a one-to-one correspondence between skew inversions for P and flip skew inversions in P^c (and a similar correspondence between flip skew inversions for P and skew inversions in P^c). The result follows directly from Theorem 3.20. \square

Remark 4.6. As explained in the proof of Theorem 4.5 the number of skew inversions of P^c is equal to the number of flip skew inversions of P . Therefore, the skew length of a conjugate path may be thought of as the skew length of the original path when flipped to a (b, a) -Dyck path.

Consider the hook lengths of the boxes in the first row of an (a, b) -core partition κ . Find the largest hook length of each residue modulo a . The a -columns of κ are the columns of κ corresponding to these hook lengths. Theorem 4.5 implies the following result, which is illustrated in Figure 10.

Corollary 4.7. *Let κ be an (a, b) -core partition. The number of boxes in the a -rows and b -boundary of κ is equal to the number of boxes in the a -columns and b -boundary of κ .*

Proof. The number of boxes in the a -rows and b -boundary of κ is equal to the skew length of κ . The number of boxes in the a -columns and b -boundary of κ is equal to the skew length of κ^c . The result then follows from Theorem 4.1 and Theorem 4.5 by applying Anderson's bijection. \square

5. THE ZETA MAP (AND ETA)

The zeta map is an intriguing map from $\mathfrak{D}_{a,b}$ to $\mathfrak{D}_{a,b}$ which can be defined in a wide variety of ways. See, for example, [AHJ14, ALW14b, ALW14a, GM14], with equivalence of many definitions given in [ALW14b]. The precise description of zeta depends on making some choices; in our experience, these choices always resolve into one of two distinct maps, which we call zeta and eta. The eta map can be interpreted as the zeta map applied to the conjugate of P , as proved in Proposition 5.5. The joint dynamics of zeta and eta will be used to present a combinatorial description of the inverse of zeta in Section 6.

In this section we present four combinatorial descriptions for computing the zeta and eta maps, starting with an interpretation involving core partitions implicit in [AHJ14], followed by with an equivalent description via the sweep maps considered in [ALW14b]. Our main contributions are two new combinatorial descriptions of the zeta map involving interval intersections and a laser filling, along with the study of the eta map in all four contexts.

5.1. Zeta and eta via cores.

Drew Armstrong conjectured a combinatorial interpretation for the zeta map by way of core partitions, drawing inspiration from Lapointe and Morse's bounded partitions [LM05], after learning of Loehr and Warrington's sweep map discussed in the next section. We present his definition and provide a parallel definition for the eta map.

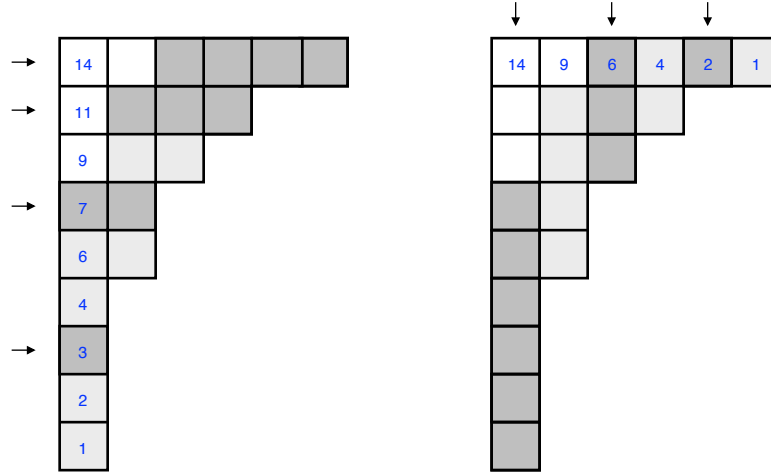


FIGURE 10. (Left) The 8-boundary boxes of our favorite $(5, 8)$ -core κ are shaded; those in the 5-rows of κ are darker. (Right) The 8-boundary boxes of κ are shaded; those in the 5-columns of κ are darker. The number of darkly shaded boxes on the left $4 + 3 + 2 + 1 = 10$ is equal to the number of darkly shaded boxes on the right $6 + 3 + 1 = 10$. (See Corollary 4.7.)

Definition 5.1. Let P be an (a, b) -Dyck path and let $\mathfrak{c}(P)$ be its corresponding (a, b) -core. From P define two partitions $\lambda(P)$ and $\mu(P)$ and corresponding lattice paths $\zeta(P)$ and $\eta(P)$:

- $\lambda(P) = (\lambda_1, \dots, \lambda_a)$ is the partition that has parts equal to the number of b -boundary boxes in the a -rows of $\mathfrak{c}(P)$.
- $\mu(P) = (\mu_1, \dots, \mu_b)$ is the partition that has parts equal to the number of a -boundary boxes in the b -rows of $\mathfrak{c}(P)$.
- $\zeta(P)$ is the (a, b) -Dyck path that bounds the partition $\lambda(P)$.
- $\eta(P)$ is the (a, b) -Dyck path that bounds the conjugate of the partition $\mu(P)$.

The *zeta map* $\zeta : \mathfrak{D}_{a,b} \rightarrow \mathfrak{D}_{a,b}$ is defined by $\zeta : P \mapsto \zeta(P)$. The *eta map* $\eta : \mathfrak{D}_{a,b} \rightarrow \mathfrak{D}_{a,b}$ is defined by $\eta : P \mapsto \eta(P)$.

One can see from the definition of zeta and eta via the sweep map described below, that $\zeta(P)$ and $\eta(P)$ are indeed paths that stay above the main diagonal. We refer to [ALW14b] for a proof.

An alternative method for calculating $\lambda(P)$ and $\mu(P)$ follows from Lemmas 3.22 and 3.23.

Lemma 5.2. *The entries of the partitions $\lambda(P)$ and $\mu(P)$ satisfy:*

- λ_i is the number of skew inversions of P involving the north level n_i .
- μ_j is the number of flip skew inversions of P involving the east level e_j .

In the $(n, n + 1)$ case, the zeta map specializes to the map studied in [Hag08] for classical Dyck paths, which sends the *dinv* and *area* statistics considered by Haiman to the *area* and *bounce* statistics considered by Haglund. One of the main interests on the zeta map is the fact that it sends skew length to co-area, or equivalently, co-skew length to area.

Corollary 5.3. *The skew length of P is equal to the co-area of $\zeta(P)$.*

Proof. The co-area of $\zeta(P)$ is by definition equal to the number of boxes in the partition λ . By Lemma 5.2, this number of boxes counts the number of skew inversions of P , and thus is equal to the skew length of P . \square

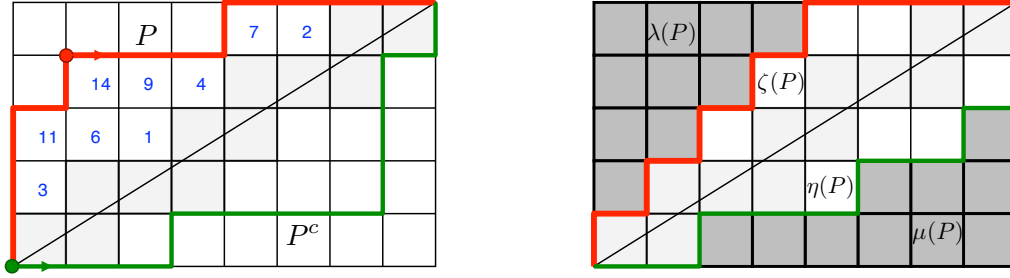


FIGURE 11. In our running example, $\zeta(P)$ bounds the partition $\lambda(P) = (4, 3, 2, 1, 0)$ and $\eta(P)$ bounds the conjugate of the partition $\mu(P) = (3, 2, 2, 1, 1, 1, 0, 0)$.

Remark 5.4. The divv statistic for classical Dyck paths can be generalized to the rational Catalan case as the number of boxes B above the path satisfying

$$\frac{\text{arm}(B)}{\text{leg}(B) + 1} \leq \frac{b}{a} < \frac{\text{arm}(B) + 1}{\text{leg}(B)},$$

where arm denotes the number of boxes directly on the right of B above the path, and leg denotes the number of boxes directly below B above the path. This intriguing statistic also satisfies $\text{divv}(P) = \text{area}(\zeta(P))$, see [LW09, Theorem 16] and [GM13]. As a consequence the co-skew length and divv statistics are the same,

$$(5.1) \quad \text{sl}'(P) = \text{divv}(P).$$

Note that the definition of divv is preserved by flipping an (a, b) -Dyck path to a (b, a) -Dyck path, and therefore skew length is preserved by flipping (as alternatively proved in Corollary 3.18). By Remark 4.6, the skew length of the conjugate of P is equal to the skew length of P when flipped to a (b, a) -Dyck path. This provides an alternative proof that skew length is preserved under conjugation (Theorem 4.5).

Proposition 5.5. *Let P be an (a, b) -Dyck path. Then*

$$\eta(P) = \zeta(P^c).$$

Proof. There is a one-to-one correspondence between the skew inversions of P^c and the flip skew inversions of P , as shown in the proof of Theorem 4.5. Through Lemma 5.2, one deduces that $\lambda(P^c)$ is the conjugate of $\mu(P)$. As a consequence, $\zeta(P^c) = \eta(P)$.

An alternative proof is presented in Section 5.2. □

Example 5.6. Figure 11 illustrates an example of the zeta map and the eta map applied to our running example path P . From Example 3.24, the 8-boundary boxes in the 5-rows of $\mathfrak{c}(P)$ give $\lambda(P) = (4, 3, 2, 1, 0)$ and the 5-boundary boxes in the 8-rows of the core $\mathfrak{c}(P)$ give $\mu(P) = (3, 2, 2, 1, 1, 1, 0, 0)$. Then $\zeta(P)$ is the path that bounds $\lambda(P)$ and $\eta(P)$ is the path that bounds the conjugate partition $\mu(P)^c = (6, 3, 1, 0, 0)$. We often combine $\lambda(P)$, $\zeta(P)$, $\mu(P)$, and $\eta(P)$ as on the right hand side of Figure 15.

The core partition $\mathfrak{c}(P^c)$ corresponding to the conjugate path P^c is illustrated in the right part of Figure 7. The a -rows of this core are the rows with leading hooks 14, 6, and 2. Counting the number of b -boundary boxes in these rows shows that $\lambda(P^c) = (6, 3, 1, 0, 0)$, which equals $\mu(P)^c$. We see that $\eta(P) = \zeta(P^c)$.

Denote by P^{flip} the result of flipping an (a, b) -Dyck path P to a (b, a) -Dyck path. The example corresponding to the path P in Figure 11 and the following result are illustrated in Figure 12.

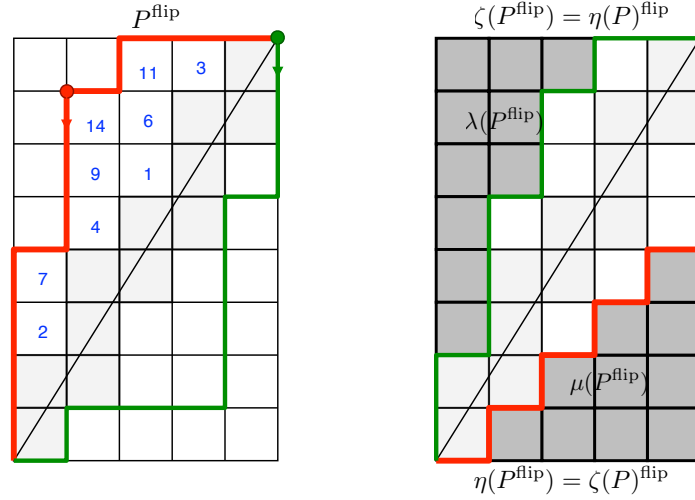


FIGURE 12. Zeta and eta applied to the flipped Dyck path of our running example path P .

Proposition 5.7. *Let P be an (a, b) -Dyck path. Then,*

$$\begin{aligned}\zeta(P^{\text{flip}}) &= \eta(P)^{\text{flip}}, \\ \eta(P^{\text{flip}}) &= \zeta(P)^{\text{flip}}.\end{aligned}$$

Proof. The skew inversions of P^{flip} are in correspondence with the flip skew inversions of P , and therefore $\lambda(P^{\text{flip}}) = \mu(P)$. As a consequence, $\zeta(P^{\text{flip}}) = \eta(P)^{\text{flip}}$. A similar argument shows that $\mu(P^{\text{flip}}) = \lambda(P)$ and $\eta(P^{\text{flip}}) = \zeta(P)^{\text{flip}}$. \square

5.2. Zeta and eta via sweep maps.

This section presents the combinatorial description of the zeta map on rational Dyck paths as a *sweep map* created by Loehr and Warrington in [ALW14b].

Heuristically, this map ‘sweeps’ the line of fixed slope $\frac{a}{b}$ across P starting on the main diagonal moving to the northwest, recording north and east steps in the order in which they are met. Analogously, the eta map ‘sweeps’ the line of slope $\frac{a}{b}$ across P starting at the farthest point from the main diagonal moving to the southeast, recording south and west steps in the order in which they are met[‡]. This procedure is illustrated for our running example in Figure 13.

Recall that the reading word $L(P)$ is obtained by reading the levels that occur along the path from southwest to northeast, excluding the final 0, and the reverse reading word $M(P)$ is obtained by reading from northeast to southwest, excluding the final 0.

Theorem 5.8 ([ALW14b]). *The zeta map can be computed as follows:*

- (1) Place a bar over each of the entries of $L(P)$ corresponding to an east step; these occur exactly at the right (cyclic) descents of σ .
- (2) Sort $L(P)$ in increasing order, keeping track of the bars on various values.
- (3) Read the resulting sequence of labels (bars and non-bars) to produce a new northeast lattice path, which we denote $\zeta(P)$.

Theorem 5.9. *The eta map can be computed as follows:*

- (1′) Place a bar over each of the entries of $M(P)$ corresponding to a west step; these occur exactly at the right (cyclic) ascents of τ .

[‡]These definitions exhibit the choice of ‘east-north’ or ‘west-south’ convention in [ALW14b].

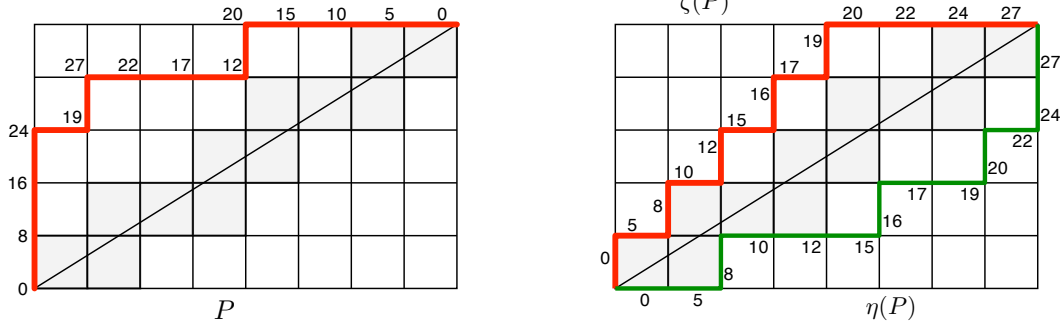


FIGURE 13. Zeta and eta via sweep maps. The steps of $\zeta(P)$ are labeled by the levels of the lattice points of P in order, recording whether they correspond to north or east levels. The steps of $\eta(P)$ are labeled by the levels of the lattice points of P in reverse order starting from the upper right corner, recording whether they correspond to south or west levels.

- (2') Sort $M(P)$ in increasing order, keeping track of the bars on various values.
- (3') Read the resulting sequence of labels (bars and non-bars) to produce a new southwest lattice path from (b, a) to $(0, 0)$, which we denote $\eta(P)$.

Example 5.10. In our running example in Figure 13, we mark the reading word

$$L(P) = (0, 8, 16, \overline{24}, 19, \overline{27}, \overline{22}, \overline{17}, 12, \overline{20}, \overline{15}, \overline{10}, \overline{5}),$$

which sorts to $(0, \overline{5}, 8, \overline{10}, 12, \overline{15}, 16, \overline{17}, 19, \overline{20}, \overline{22}, \overline{24}, \overline{27})$. Thus $\zeta(P)$ is the path

$$NENENENENEEEE.$$

We mark the reverse reading word

$$M(P) = (\overline{0}, \overline{5}, \overline{10}, \overline{15}, 20, \overline{12}, \overline{17}, \overline{22}, 27, \overline{19}, 24, 16, 8),$$

which sorts to $(\overline{0}, \overline{5}, 8, \overline{10}, \overline{12}, \overline{15}, 16, \overline{17}, \overline{19}, 20, \overline{22}, 24, 27)$. Thus $\eta(P)$ is the path

$$WWSWWSWWSWSS, \text{ which is equivalent to } NNENEENEENE.$$

Remark 5.11. Note that both computations in Theorem 5.8 and Theorem 5.9 can be performed just as easily on the standardization $\sigma(P)$ of $L(P)$, since only the relative values of the labels matter.

Proof of Theorems 5.8 and 5.9. Consider the path $\zeta(P)$ described in Theorem 5.8. The number of boxes on the left of the north step corresponding to a north level n_i of P is equal to the number of east levels smaller than n_i . This number is equal to the number of skew inversions involving n_i , which coincides with λ_i by Lemma 5.2 (i). Therefore the described algorithm to compute $\zeta(P)$ coincides with the definition of zeta in Definition 5.1.

Consider the (rotation of the) path $\eta(P)$ described in Theorem 5.9. The number of boxes below a given west step of P is equal to the number of south levels smaller than the corresponding west level. This number is equal to the number of flip skew inversions involving the corresponding level e_j , which coincides with μ_j by Lemma 5.2 (ii). Therefore, the described algorithm to compute $\eta(P)$ coincides with the definition of eta in Definition 5.1. \square

Using the description of zeta and eta in terms of sweep maps, we have the following alternative proof of Proposition 5.5, which states that $\eta(P) = \zeta(P^c)$.

Alternative proof of Proposition 5.5. The conjugate of P is obtained by applying a cyclic shift on P and then rotating the diagram 180° . As a result, the levels appearing in the reading word of P^c

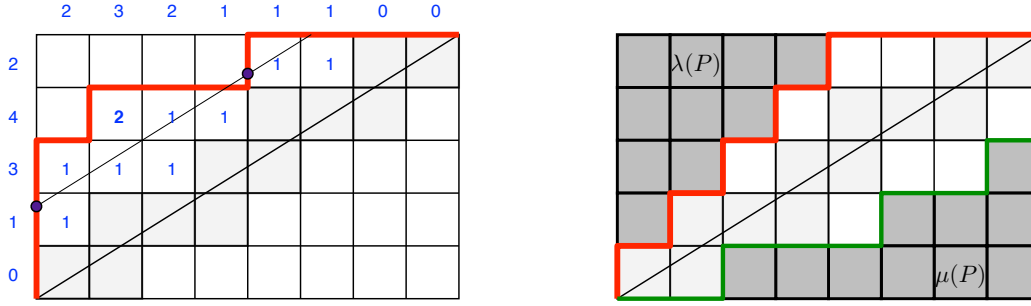


FIGURE 14. Laser filling of a path P . The laser pointed from the lower right corner of the box with filling 2 crosses two vertical walls of the path, while all other lasers cross only one. The entries of the partition $\lambda(P) = (4, 3, 2, 1, 0)$ are the sums of the laser fillings on the rows. The entries of the partition $\mu(P) = (3, 2, 2, 1, 1, 1, 0, 0)$ are the sums of the laser fillings on the columns.

appear in the opposite order in which they appear in the reading word of P , though cyclically shifted. Furthermore, the east levels are transformed into west levels and the north levels into south, transforming the step (1) of the algorithm into step (1'). The cyclic shift changes all of the levels in the reading word by the same amount, so this shift has no impact on the sorting operation performed in the second step. \square

5.3. Zeta and eta via the laser filling.

This section presents a new interpretation of zeta and eta that are read from a *laser filling* in the boxes below the path P and above the main diagonal. Our main result in this section describes the partitions λ and μ in terms of the laser filling. This result will be used in Section 7 to give a new beautiful combinatorial description of the inverse of the zeta map in the square case without the use of bounce paths.

Figure 14 illustrates the following definition.

Definition 5.12. Let P be an (a, b) -Dyck path and let B be a box below P and above the line $y = \frac{a}{b}x$. Draw the line of slope $\frac{a}{b}$ through the southeast corner of B (a bi-directional laser). The *laser filling* of B is equal to the number of vertical walls of P crossed by the laser. Equivalently, it is equal to the number of horizontal walls of P crossed by the laser.

Remark 5.13. Lasers also appear in Armstrong, Rhoades, and Williams's [ARW13]. Their lasers stop at the first wall they meet; by contrast, our lasers traverse (and count!) the walls of the path P .

Theorem 5.14. *The partitions λ and μ associated to P can be computed as follows:*

- (i) *The entries of $\lambda(P)$ are the sums of the laser fillings in the rows.*
- (ii) *The entries of $\mu(P)$ are the sums of the laser fillings in the columns.*

Proof. The entries of λ count the skew inversions involving the north levels of each of the vertical steps in the path. For a given vertical step, this number is equal to the number of horizontal steps in the path that are strictly below the laser through its starting point. Each of these horizontal steps is crossed by exactly one of the lasers through the lower right corners of the boxes below the path that are in the same row of the vertical step in consideration. The statement (i) follows. The other part is proved similarly. \square

Corollary 5.15. *The skew length of P is equal to the sum of the laser fillings of P .*

Proof. The skew length of P is equal to the area of $\lambda(P)$. By the previous theorem, this area is equal to the sum of all laser fillings of P . \square

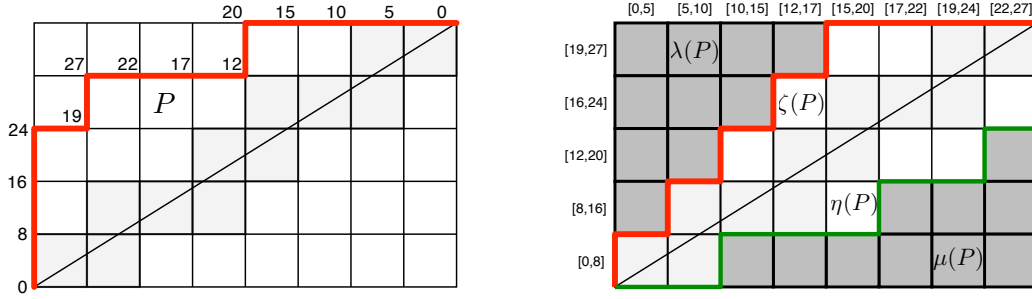


FIGURE 15. Zeta and eta via interval intersections. The intervals on the left correspond to the ordered level intervals of the vertical steps in the path. The intervals on the top correspond to the level intervals of the horizontal steps. The shaded boxes of λ and μ are the boxes whose corresponding row and column intervals do not intersect.

5.4. Zeta and eta via interval intersections.

This section presents a second new combinatorial interpretation of zeta and eta in terms of *interval intersections*. Each step of the path P has an associated closed interval whose endpoints are the levels of its starting and ending points. When the intervals are ordered in increasing order, zeta and eta can be directly determined.

Definition 5.16. Let P be an (a, b) -Dyck path. Let $N(P)$ be the north levels of P and $E(P)$ be the east levels of P . Define the *north intervals* of P to be the set $\mathcal{I}_N = \{[n_i, n_i + b] \text{ for } n_i \in N(P)\}$ and the *east intervals* of P to be the set $\mathcal{I}_E = \{[e_j - a, e_j] \text{ for } e_j \in E(P)\}$.

Theorem 5.17. Create an $a \times b$ grid. Label the rows of the grid by the north intervals of P increasing from bottom to top, and the columns of the grid by the east intervals of P increasing from left to right. Fill in the boxes in this grid when the corresponding row and column intervals do not intersect. The boundary path of the shaded boxes above the main diagonal is $\zeta(P)$ and the boundary path of the shaded boxes below the main diagonal is $\eta(P)$, rotated 180 degrees.

Proof. This theorem is a straightforward consequence of Lemma 5.2. \square

Example 5.18. For our running example path P , the north intervals are $[0, 8]$, $[8, 16]$, $[12, 20]$, $[16, 24]$, and $[19, 27]$, which can be read directly from the north steps of P , or calculated from the north levels as in Definition 5.16. Similarly, the east intervals of P are $[0, 5]$, $[5, 10]$, $[10, 15]$, $[12, 17]$, $[15, 20]$, $[17, 22]$, $[19, 24]$, and $[22, 27]$. Labeling the rows of a 5×8 grid with the north levels and the columns with the east levels gives the right side of Figure 15. The shaded boxes are the those where the corresponding row interval does not intersect the corresponding column interval, from which $\lambda(P)$, $\mu(P)$, $\zeta(P)$, and $\eta(P)$ can be read posthaste.

6. PAIRING THE ZETA MAP WITH THE ETA MAP

By considering the zeta map together with the eta map, we gain two new ideas: a new approach for proving that the zeta map is a bijection and (if ζ is a bijection) a new area-preserving involution on the set of (a, b) -Dyck paths. For clarity and consistency, we have decided to use the letter P to denote a path that is in the domain of ζ and use the letter Q to denote a path that is in the image of ζ .

6.1. Inverse of the zeta map knowing eta.

For the image \mathfrak{J} under the pair of maps

$$(\zeta, \eta) : \mathfrak{D} \rightarrow \mathfrak{D} \times \mathfrak{D},$$

we define a map $\iota : \mathfrak{Z} \rightarrow \mathfrak{D}$ such that $(\zeta, \eta) \circ \iota$ is the identity map. Further, we conjecture that for every (a, b) -Dyck path Q that appears as the image of ζ , there exists a unique (a, b) -Dyck path R such that $(Q, R) \in \mathfrak{Z}$. This would imply that in \mathfrak{Z} every element of \mathfrak{D} appears exactly once as the initial entry in the pair, from which it would follow that the zeta map is a bijection.

Definition 6.1. A pair of (a, b) -Dyck paths (Q, R) is an *admissible pair* if $(Q, R) = (\zeta(P), \eta(P))$ for some (a, b) -Dyck path P . The *set of admissible pairs* $\mathfrak{Z} \subset \mathfrak{D} \times \mathfrak{D}$ is the image under the pair of maps $(\zeta, \eta) : \mathfrak{D} \rightarrow \mathfrak{D} \times \mathfrak{D}$.

We now describe a simple combinatorial description of the inverse map ι that recovers P from the pair (Q, R) or, equivalently, from the pair of partitions (λ, μ) they bound.

Definition 6.2. Let (Q, R) be an admissible pair. Define $\iota(Q, R)$ as follows.

- (1) Draw the path Q above the diagonal and rotate the path R 180 degrees so that it embeds below the diagonal in the same diagram. Label the steps of each path from 1 to $a + b$ starting at the bottom-left corner and ending at the top-right corner in the order in which they appear in the path.
- (2) Create the permutation $\gamma : [a + b] \rightarrow [a + b]$ as follows. If l is a label of an horizontal step in Q , define $\gamma(l)$ to be the label of the horizontal step in R that is in the same column of l . If l is a label of a vertical step in Q , define $\gamma(l)$ to be the label of the vertical step in R that is in the same row of l .
- (3) For admissible pairs (Q, R) , γ is a cycle permutation. Interpret γ in cycle notation as $(\sigma_1, \sigma_2, \dots, \sigma_{a+b})$, fixing $\sigma_1 = 1$. Define $P = \iota(Q, R)$ to be the path whose east steps correspond to the cyclic descents of σ .[§]

Theorem 6.3. γ is a cycle permutation and the map ι is the inverse map for the pair (ζ, η) .

Proof. Suppose (Q, R) is an admissible pair, so that there exists a $P \in \mathfrak{D}$ such that $(Q, R) = (\zeta(P), \eta(P))$. Label the steps of Q and R with the levels of P as determined by the sweep map algorithm given in Theorems 5.8 and 5.9 (as illustrated in Figure 13). The definition of the permutation γ using these labels instead of on $[a + b]$ induces a permutation on the set of levels of the lattice points of P . We will prove that this permutation is the cycle permutation given by the reading word $L(P)$ of P .

Because of the relationship between the forward reading word $L(P)$ and the reverse reading word $M(P)$, the labels of the vertical steps of R are exactly the labels of the vertical steps of Q plus b , while the labels of the horizontal steps of R are exactly the labels of the horizontal steps of Q minus a . This implies that the permutation γ maps the level of a lattice point in P to the level of the next lattice point along P , forming a permutation on the set of labels that is a cycle ordered by the reading word $L(P)$.

Since the level labels appear in order as we walk along Q , only the relative order of the labels matters; returning all labels to the numbers from 1 up to $a + b$ recovers $\gamma(P)$, which when interpreted as a permutation in one line notation is the reading permutation $\sigma(P)$. By Remark 2.3, we recover P directly from $\sigma(P)$ and the result follows. \square

Taken with Theorem 6.3, the following conjecture would imply that ζ is a bijection.

Conjecture 6.4. Suppose that $Q \in \mathfrak{D}_{a,b}$. There exists at most one $R \in \mathfrak{D}_{a,b}$ such that $(Q, R) \in \mathfrak{Z}$.

Example 6.5. Figure 16 illustrates the procedure outlined in Definition 6.2 for the pair $(Q, R) = (\zeta(P), \eta(P))$ from our running example P . After labeling the paths $Q = \zeta(P)$ and $R = \eta(P)$ from 1 to 13, we see that $\gamma(1) = 3$, $\gamma(2) = 1$, $\gamma(3) = 7$, etc. Writing γ in cycle notation gives

$$\gamma = (1, 3, 7, \mathbf{12}, 9, \mathbf{13}, \mathbf{11}, \mathbf{8}, 5, \mathbf{10}, \mathbf{6}, \mathbf{4}, \mathbf{2}).$$

[§]A descent occurs when $\sigma_i > \sigma_{i+1}$. A cyclic descent is defined in the same way, but considering the indices modulo $a + b$, allowing a descent in the last position of σ .

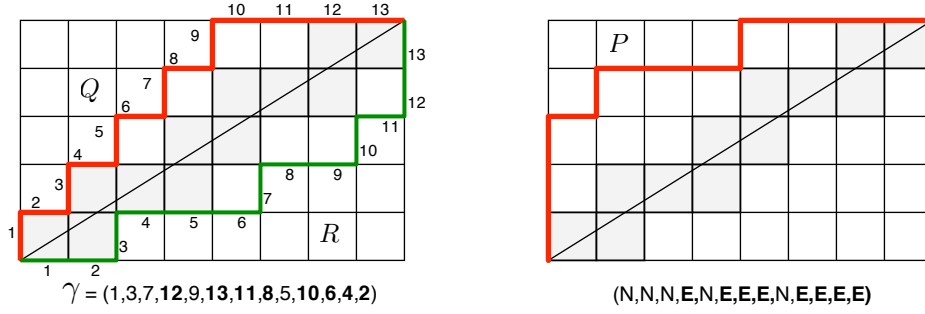


FIGURE 16. Calculating $P = \iota(Q, R)$ using the method in Definition 6.2.

If we instead interpret this sequence of numbers as the one line notation of a permutation σ , the cyclic descents of σ are bolded and correspond to the east steps of $\iota(Q, R)$. We see that $\iota(Q, R) = P$.

Remark 6.6. The essence of the proof of Theorem 6.3 is that the ζ and η maps track the positions of the right cyclic descents of $L(P)$ and $M(P)$. Using these two sets of data, and the precise relationship between $L(P)$ and $M(P)$, we are able to solve for the levels of P . Interestingly, $\zeta(P)$ does not obviously contain enough information to reconstruct P . We cannot construct a unique permutation solely from its collection of right descents, and need additional information to recover P . In the standard Catalan case, this additional information is essentially implied by the particular structure of the $n \times (n+1)$ rectangle; for the general case, we obtain the extra information necessary from $\eta(P)$.

6.2. An area-preserving involution on rational Dyck paths.

If ζ is invertible, we can use η to define a new area-preserving involution on the set of (a, b) -Dyck paths, induced by the conjugate map under ζ which we call the conjugate-area map. This involution sends the path $\zeta(P)$ to the path $\eta(P) = \zeta(P^c)$ and is predictable for certain families of (a, b) -Dyck paths.

Definition 6.7. The conjugate-area map applied to an (a, b) -Dyck path Q is the path

$$\chi(Q) := \zeta \circ c \circ \zeta^{-1}(Q).$$

If λ is the partition bounded by Q , we define $\chi(\lambda)$ to be the partition bounded by $\chi(Q)$.

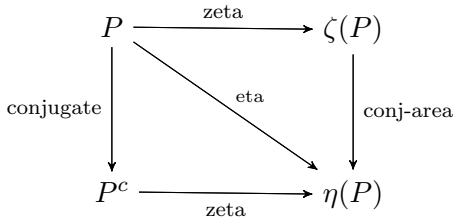


FIGURE 17. Diagrammatic description of the conjugate-area involution.

Remark 6.8. For partitions λ and μ bounded by $\zeta(P)$ and $\eta(P)$ we have $\chi(\lambda) = \mu^c$.

Proposition 6.9. If the zeta map is a bijection then the conjugate-area map is an area-preserving involution on the set of (a, b) -Dyck paths.

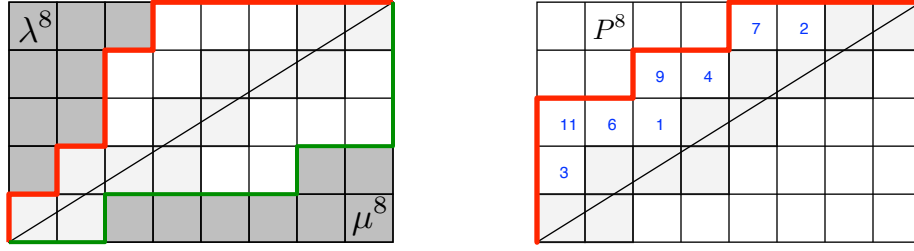


FIGURE 18. The left-justified and up-justified partitions $\chi(\lambda^n) = (\mu^n)^c$ and their corresponding path P^n for $n = 8$.

Proof. Since conjugation is an involution, we see that applying the operator $\zeta \circ c \circ \zeta^{-1}$ twice is equal to the identity, and therefore $\chi(\chi(Q)) = Q$. Furthermore, conjugation preserves skew length (Theorem 4.5), which is mapped to co-area via the zeta map. Thus, χ must be an area-preserving involution. \square

One possible approach to prove that ζ is a bijection would be to directly construct the involution χ . In Section 7 we show that in the square case χ is exactly the map that reverses the path P ; equivalently one finds $\chi(\lambda)$ by simple conjugation. In the rational case, conjugation must fail in general because conjugates of partitions may not sit above the main diagonal. Although, Proposition 6.11 exhibits our empirical observation that for ‘small’ partitions λ , $\chi(\lambda)$ is often the conjugate.

We have found that χ is predictable in other families of examples as well; in Section 8 we present an inductive combinatorial description of the inverse of the zeta map and of the area-preserving involution for a nice family of examples.

Example 6.10 (Left-justified and up-justified partitions). Consider two families of partitions whose Young diagrams fit above the main diagonal in the $a \times b$ grid. Let $n \in \mathbb{N}$ be a number no bigger than the number of boxes above the main diagonal in the $a \times b$ grid. Define the *left-justified partition* λ^n to be the partition whose Young diagram has n boxes as far to the left as possible and the *up-justified partition* μ^n to be the partition whose Young diagram has n boxes as far up as possible. Figure 18 shows λ^8 embedded above the diagonal and μ^8 rotated 180 degrees and embedded below the diagonal.

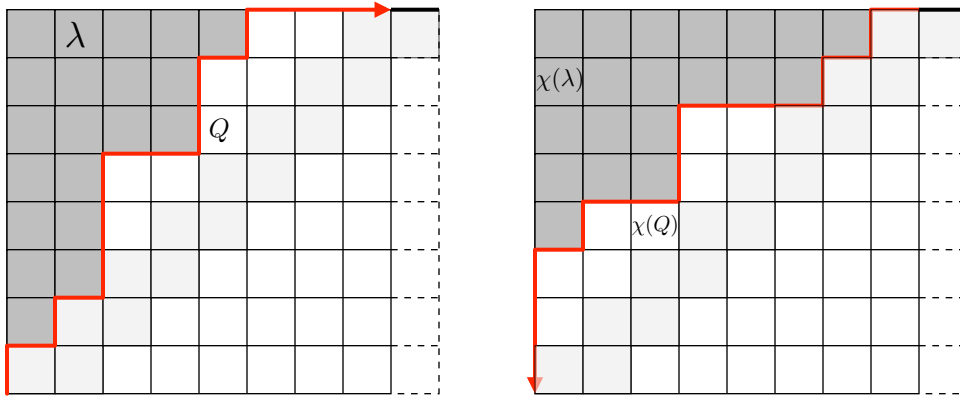
Proposition 6.11. *The left-justified and up-justified partitions are related by the conjugate-area map:*

$$\chi(\lambda^n) = (\mu^n)^c.$$

Moreover, $\zeta^{-1}(\lambda^n)$ is the path with area n containing the first n positive hooks in the grid.

Proof. Let P^n be the path containing the first n positive hooks in the grid. This path consists of all the boxes below a line parallel to the main diagonal sitting in the highest level of the path, and therefore all the labels in the laser filling are equal to 1. Adding the labels in the rows and the columns we obtain the partitions λ^n and μ^n . \square

Figure 18 illustrates an example of left-justified and up-justified partitions λ^n and μ^n together with their corresponding path P^n for $n = 8$. The reader is invited to verify that $\zeta(P^8)$ and $\eta(P^8)$ are given by the paths bounded by λ^8 and μ^8 using any of the methods described in Section 5, as well as to verify that the inverse map ι presented in Section 6 gives P^8 when applied to the paths bounding λ^8 and μ^8 .

FIGURE 19. The conjugate-area involution in the $(n, n + 1)$ case.

7. THE SQUARE CASE

In this section, we consider $(n, n + 1)$ -Dyck paths, lattice paths in an $n \times (n + 1)$ grid staying above the main diagonal. They are in bijection with classical Dyck paths in an $n \times n$ grid by simply forgetting the last east step of the path. Haglund and Haiman [Hag08] discovered a beautiful description of the inverse of the zeta map in this case using a bounce path that completely characterizes the area sequence below the path. We present a new combinatorial description of the inverse of the zeta map in this case in terms of an area-preserving involution. This approach opens a new direction in proving that the zeta map is a bijection in the general (a, b) case.

7.1. The conjugate-area involution, conjugate partitions and reverse paths.

Let Q be an $(n, n + 1)$ -Dyck path. The area-preserving involution χ conjugates the partition λ bounded by the path Q . For simplicity, denote by Q^r the path whose bounded partition is λ^c . We refer to P^r as the *reverse path* of Q . Forgetting the last east step of the path, the reverse operation acts by reversing the path in the $n \times n$ grid. An example of the conjugate-area involution, conjugate partition and reverse path is illustrated in Figure 19.

Theorem 7.1. *For a Dyck path Q and the partition λ it bounds, we have $\chi(Q) = Q^r$ and $\chi(\lambda) = \lambda^c$.*

Proof. We need to show that the partitions λ and μ bounded by the images $\zeta(P)$ and $\eta(P)$ of any $(n, n + 1)$ -Dyck path P satisfy

$$\chi(\lambda) = \mu^c = \lambda^c.$$

Equivalently, we need to show that $\lambda = \mu$. The entries of the partitions λ and μ are the sums of the labels in the laser filling of P over the rows and columns respectively (Theorem 5.14). We will show that the values of the sums over the rows are in correspondence with the values of the sums over the columns, and therefore $\lambda = \mu$. This correspondence is illustrated for an example in Figure 20.

For every row, draw a line of slope 1 in the northeast direction pointing from the starting point of the north step in that row. This line hits the path for the first time in the ending point of an east step of the path. The labels of the laser filling in the boxes in the column corresponding to this east step are exactly the same as the labels of the laser filling in the row in consideration. (This is because the lasers are lines with slope $\frac{n}{n+1}$, which implies that for any two boxes on the same diagonal of slope 1 that are not interrupted in line of sight by the path P , they will have the same laser filling.) Thus, their corresponding sums are equal. Doing this for all the rows gives the desired correspondence between the entries of the partition λ and the entries of the partition μ . \square

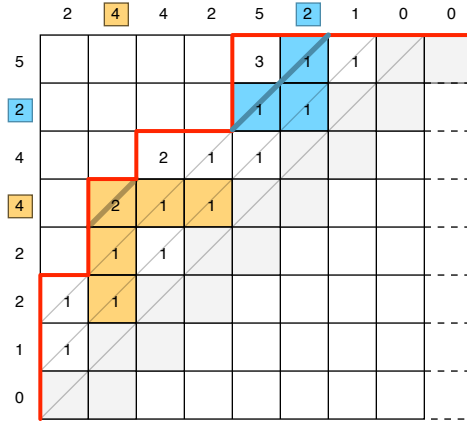


FIGURE 20. Argument in the proof of Theorem 7.1. The values of the sums over the rows are in correspondence with the values of the sums over the columns, and therefore $\lambda = \mu$.

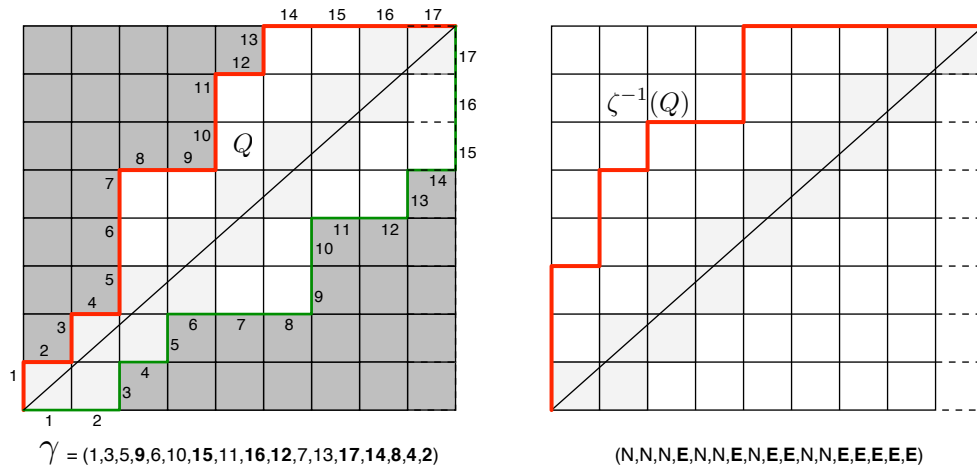


FIGURE 21. The inverse of ζ by way of conjugate partitions.

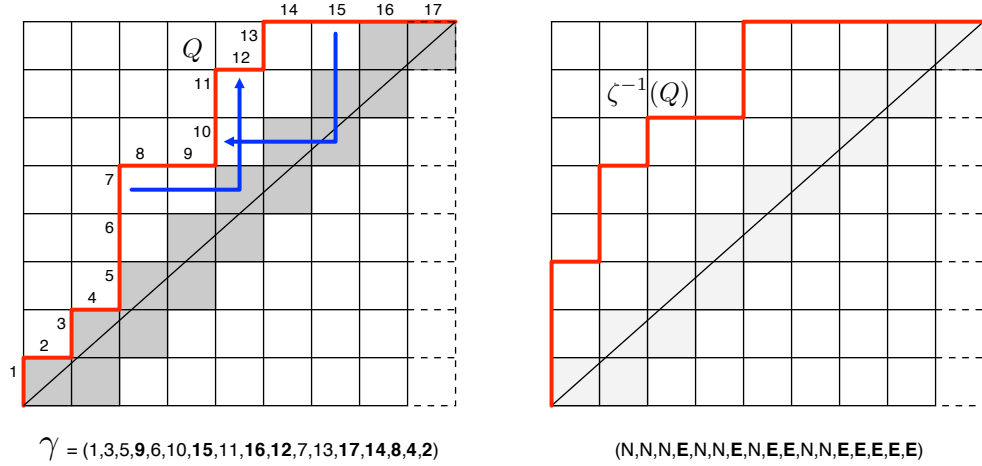
7.2. The inverse of the zeta map.

Now that Theorem 7.1 provides the explicit formula for χ , the method to find inverse of the zeta map in the $(n, n + 1)$ case follows as a direct consequence of Theorem 6.3. The description of the map ι is presented in Definition 6.2.

Theorem 7.2. *Let Q be an $(n, n + 1)$ -Dyck path. Then, $\zeta^{-1}(Q) = \iota(Q, Q^r)$.*

An example of this result is illustrated in Figure 21. The laser filling of the path $\zeta^{-1}(Q)$ in this example is shown in Figure 20. One can verify that the sum of the labels of the laser filling on the rows and columns gives rise to the partitions λ and μ bounded by Q and $\chi(Q)$ (Theorem 5.14).

An alternative way to obtain the cycle permutation γ directly from Q is as follows. Shade the boxes in the $n \times (n + 1)$ rectangle that are crossed by the main diagonal as illustrated in Figure 22. Move east from a vertical step labeled i until the center of the first shaded box you see, and then move up until hitting an horizontal step of the path. The image $\gamma(i)$ is equal to the label of this horizontal step plus 1. In the example of Figure 22, the path starting at the vertical step labeled 7 hits the horizontal step 12, therefore $\gamma(7) = 12 + 1 = 13$.

FIGURE 22. Alternative description of the cycle permutation γ .

In order to determine $\gamma(i)$ of a label of an horizontal step, we move down until the center the last shaded box we see, and then move left until hitting a vertical step of the path. As before, $\gamma(i)$ is equal to the label of this vertical step plus 1. In the example, $\gamma(15) = 10 + 1 = 11$. The image of the label of the first horizontal step of the path is by definition equal to 1. Interpret γ in cycle notation as $(\sigma_1, \sigma_2, \dots, \sigma_{2n+1})$ where we fix $\sigma_1 = 1$. As a direct consequence of Theorem 7.2 we get:

Theorem 7.3. *Let Q be an $(n, n+1)$ -Dyck path. The inverse $\zeta^{-1}(Q)$ is the path whose east steps correspond to the cyclic descents of the permutation γ when interpreted in one line notation.*

8. ZETA INVERSE AND AREA-PRESERVING INVOLUTION FOR A NICE FAMILY OF EXAMPLES

In this section we present an inductive combinatorial description of the inverse of the zeta map and of the conjugate-area involution χ for a nice family of (a, b) -Dyck paths. This family consists of the Dyck paths that contain the lattice point with level 1. Such Dyck paths are obtained by concatenating two Dyck paths in the $a' \times b'$ and $a'' \times b''$ rectangles illustrated in Figure 23. The sides of these two rectangles are the unique positive integers $0 < a', a'' < a$ and $0 < b', b'' < b$ such that

$$\begin{aligned} a'b - b'a &= 1, \\ b''a - a''b &= 1. \end{aligned}$$

As a consequence, a' and b' are relatively prime as well as a'' and b'' , allowing us to apply induction.

8.1. Zeta inverse. Let P be an (a, b) -Dyck path congaing the lattice point at level 1, and let P' and P'' be the two Dyck paths in the $a' \times b'$ and $a'' \times b''$ rectangles whose concatenation is equal to P . Define the *star product* of $P' \star P''$ as the path obtained by cutting P' at its highest level and infixing P'' . This special product is illustrated in Figure 24. Note that the highest level of P' can be equivalently obtained by sweeping the main diagonal of either the $a \times b$ rectangle or the $a' \times b'$ rectangle.

Theorem 8.1. *If Q is an (a, b) -Dyck path containing the lattice point at level 1, zeta inverse of Q is equal to the star product of the zeta inverses of Q' and Q'' :*

$$\zeta^{-1}(Q) = \zeta^{-1}(Q') \star \zeta^{-1}(Q'').$$

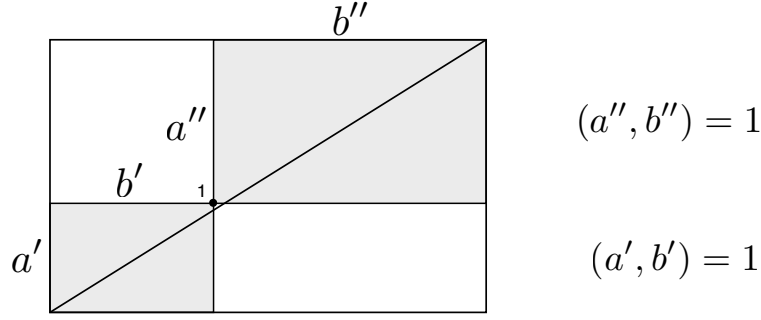


FIGURE 23. Base induction for zeta inverse and the area-preserving involution.

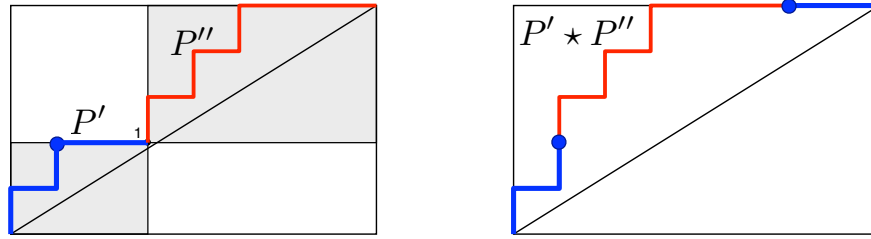


FIGURE 24. Star product of rational Dyck paths.

Proof. We will show that $\zeta(P' \star P'')$ is the concatenation of $\zeta(P')$ and $\zeta(P'')$, the theorem then follows by applying zeta to both sides of the equation. Since the path P' is cut at its highest level, sweeping the main diagonal of the $a \times b$ rectangle crosses the levels of $P' \star P''$ corresponding to the path P' first, followed by all the levels corresponding to the path P'' . Therefore, $\zeta(P' \star P'')$ is the concatenation of $\zeta(P')$ and $\zeta(P'')$. \square

8.2. Area-preserving involution. The conjugate-area map of Q can be obtained by induction in this case as well.

Lemma 8.2. *Let l be the level of a lattice point p in the $a \times b$ grid. If U_l is the rectangle composed by the boxes northwest of p and \tilde{U}_l is the rectangle composed by the boxes southeast of p , then*

$$\text{area}(\tilde{U}_l) - \text{area}(U_l) = l.$$

Proof. If $p = (p_1, p_2)$, then $l = p_2b - p_1a$. Furthermore,

$$\text{area}(\tilde{U}_l) - \text{area}(U_l) = (b - p_1)p_2 - p_1(a - p_2) = p_2b - p_1a = l.$$

\square

Theorem 8.3. *Let Q is an (a, b) -Dyck path containing the lattice point at level 1. The bounded partition of $\chi(Q)$ is the partition whose restriction to the $a' \times b'$ and $a'' \times b''$ rectangles gives the bounded partitions of $\chi(Q')$ and $\chi(Q'')$, and which contains all boxes below the main diagonal outside the two rectangles.*

Proof. We first observe that $\chi(Q)$ defined this way has the same area of Q . This is equivalent to show that the bounded partitions of $\chi(Q)$ and Q have the same area, when restricted to the complement of the $a' \times b'$ and $a'' \times b''$ rectangles. These restrictions are exactly the rectangle \tilde{U}_1 after removing the box on its upper left corner, and the rectangle U_1 . The claim then follows by Lemma 8.2.

Now, let γ' and γ'' be the cycle permutations arising from the pairs $(Q', \chi(Q'))$ and $(Q'', \chi(Q''))$, and γ be the cycle permutation of $(Q, \chi(Q))$. The cycle permutation γ can be obtained by cutting γ'

exactly before its highest value and putting γ'' in between, with all its values increased by $a' + b'$. In the example in Figure 25 we get

$$\begin{aligned}\gamma' &= (1, 3 \mid 5, 4, 2) \\ \gamma'' &= (1, 3, 7, 5, 8, 6, 4, 2) \\ \gamma &= (1, 3, 6, 8, 12, 10, 13, 11, 9, 7, 5, 4, 2)\end{aligned}$$

The cyclic descents of γ correspond exactly to the cyclic descents of γ' and γ'' . Moreover, the descent at the highest value of γ' corresponds to the east step at the highest level of $\zeta^{-1}(Q')$. Thus, replacing cyclic descents in γ by east steps and ascents by north steps gives rise to the start product $\zeta^{-1}(Q') \star \zeta^{-1}(Q'')$, which is equal to $\zeta^{-1}(Q)$ by Theorem 8.1. \square

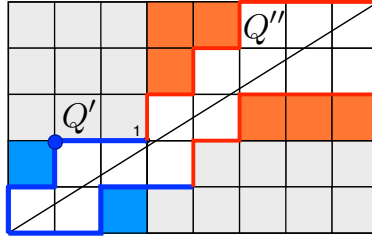


FIGURE 25. The inductive conjugate-area map for paths containing level 1.

8.3. k th valley Dyck paths. One interesting family of (a, b) -Dyck paths is the family of k th valley Dyck paths, paths Q_k with valleys at levels $0, 1, 2, \dots, k$ for some $k < a$. The area-conjugate map for these paths behaves very nice and can be described in terms of the rectangles U_l and \tilde{U}_l in Lemma 8.2.

For $0 < l < a$, consider the collections of boxes V_l and \hat{V}_l defined by

$$V_l = U_l \setminus \bigcup_{i=1}^{l-1} U_i, \quad \hat{V}_l = \hat{U}_l \setminus \bigcup_{i=1}^{l-1} \hat{U}_i,$$

where \hat{U}_i is composed of the boxes of \tilde{U}_i that are below the main diagonal. Equivalently, \hat{U}_i is the result of removing the box in the upper left corner of \tilde{U}_i . An example is illustrated in Figure 26.

Lemma 8.4. *For $0 < l < a$, the area of V_l is equal to the area of \hat{V}_l .*

Proof. Since $V_1 = U_1$ and $\hat{V}_1 = \hat{U}_1$, which is \tilde{U}_1 after removing one box, Lemma 8.2 implies that V_1 and \hat{V}_1 have the same area. The level 2 becomes level 1 in the smaller $a'' \times b''$ rectangle, and V_2, \hat{V}_2 are given by U_1, \hat{U}_1 in this smaller rectangle. Again, Lemma 8.2 implies that V_2 and \hat{V}_2 have the same area. Continuing the same argument in the smaller rectangles that appear in the process finishes the proof. \square

Note that the bounded partition of Q_k is the (disjoint) union of V_1, \dots, V_k .

Proposition 8.5. *The bounded partition of $\chi(Q_k)$ is the (disjoint) union of $\hat{V}_1, \dots, \hat{V}_k$.*

Proof. Note that the restriction of Q_k to the $a' \times b'$ and $a'' \times b''$ rectangles gives two smaller k th valley Dyck paths $Q'_{k'}$ and $Q''_{k''}$. The result then follows directly from Theorem 8.3 by induction on k . \square

Figure 27 illustrates an example of the inverse of the zeta map for k th valley Dyck paths obtained by applying Theorem 6.3.

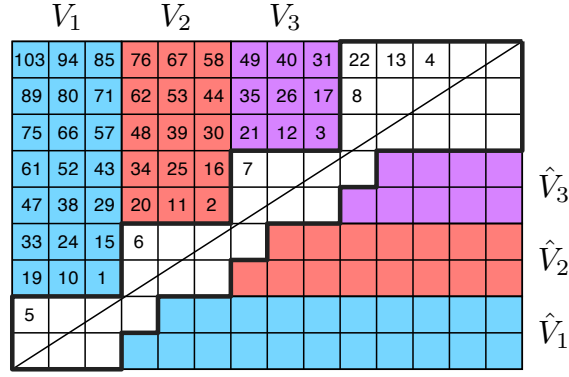


FIGURE 26. Example of the conjugate-area map for k th valley Dyck paths for $k = 3$. The area of V_i is equal to the area \hat{V}_i .

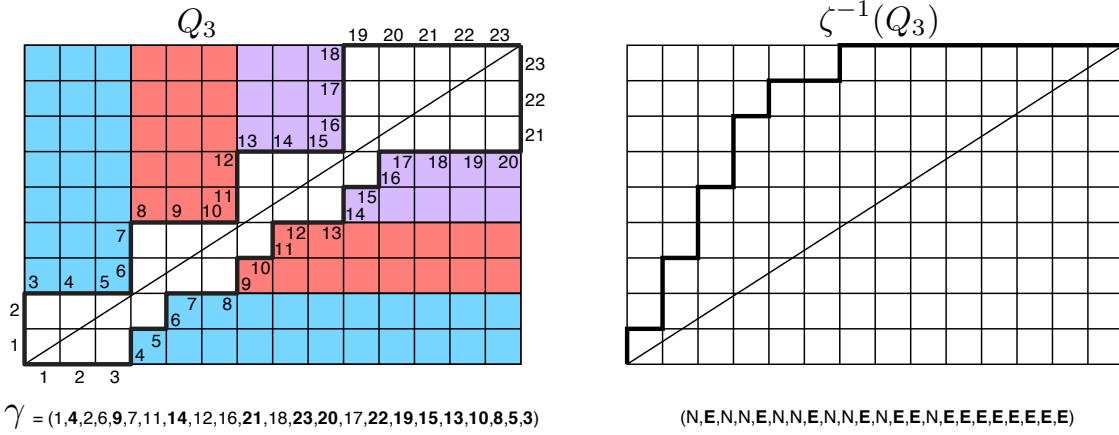


FIGURE 27. Example of the inverse of the zeta map for k th valley Dyck paths for $k = 3$.

9. TOWARDS THE BIJECTION

We have tried a number of approaches for showing that ζ itself is a bijection, without success. In this section, we detail some of our approaches which are combinatorially interesting and may play a role in an eventual proof.

9.1. Characterizing permutations.

We first focus on the permutations $\sigma(P)$ and $\gamma(P)$, which fully encode P , $\zeta(P)$, and $\eta(P)$.

The *exceedences* of $\gamma(P)$ encode both $\zeta(P)$ and $\eta(P)$ by way of their positions and values. If i and j are adjacent entries of $\sigma(P)$ with $i < j$, then in $\gamma(P)$ we have $i < j = \gamma(i)$, which is exactly an exceedence. Ascents in $\sigma(P)$ encode north steps of P , so this exceedence tells us that the i th step of $\zeta(P)$ is a north step. As such, the *positions* of the exceedences in $\gamma(P)$ encode $\zeta(P)$.

Similarly, the *values* of the exceedences of $\gamma(P)$ encode $\eta(P)$. In fact, if we draw the path whose north steps are given by the values of the exceedences of $\gamma(P)$, we will obtain a path strictly below the diagonal which may be rotated to obtain $\eta(P)$. This correspondence is clear from the method for computing P from $\zeta(P)$ and $\eta(P)$ in Section 6.1, see Figure 16.

Proposition 9.1. *The positions of the exceedences of $\gamma(P)$ give the collection of north steps in $\zeta(P)$, and the values of the exceedences of $\gamma(P)$ are the north steps in $\eta(P)$ when rotated 180°.*

Example 9.2. The permutations $\sigma(P)$ and $\gamma(P)$ for our running example path P in Figure 1 are

$$\sigma(P) = [1, 3, 7, 12, 9, 13, 11, 8, 5, 10, 6, 4, 2]$$

and

$$\begin{aligned}\gamma(P) &= (1, 3, 7, 12, 9, 13, 11, 8, 5, 10, 6, 4, 2) \\ &= [3, 1, 7, 2, 10, 4, 12, 5, 13, 6, 8, 9, 11].\end{aligned}$$

Recall that square brackets are used for one-line notation and round parentheses for cycle notation. The excedences of γ are at positions $\{1, 3, 5, 7, 9\}$, which are exactly the north steps of $\zeta(P)$ illustrated as the path Q in Figure 16. The values of $\gamma(P)$ at these positions are $\{3, 7, 10, 12, 13\}$, which are precisely the north steps of $\eta(P)$ illustrated as the path R in Figure 16.

We can directly construct the conjugate map on the level of permutations algebraically. Recall that the inverse map on permutations exchanges the roles of values and positions. Let ω_0 be the longest element of S_{a+b} . Then one may check that

$$\gamma(P^c) = \omega_0 \gamma(P)^{-1} \omega_0.$$

This involution exchanges $\zeta(P)$ and $\eta(P)$, but does not tell us how to construct $\zeta(P)$ directly from $\eta(P)$. We expect that a strong combinatorial characterization of the permutations γ that arise from an actual path P would give an understanding of the conjugate-area map, and thus allow the bijection to be proven.

Recall from Section 6.1 that we can read $\gamma(P)$ from the diagram embedding $\zeta(P)$ above the diagonal and $\eta(P)$ below the diagonal. Given any two (a, b) -Dyck paths, we could embed them together in a diagram, one playing the role of Q and the other playing the role of R . The resulting diagram yields a permutation γ , and we naturally ask whether this γ actually arises as $\gamma(P)$ for some path P . The answer, of course, is almost always no: a strong characterization of legal pairs of paths would yield a direct description of the conjugate-area map.

When pairing arbitrary Q and R paths a number of things can go wrong. First, Theorem 4.5 implies that in order to come from an actual path, we must have $\text{area}(Q) = \text{area}(R)$. Second, we know that γ must have a single cycle; it is simple to construct examples where this does not occur. It is also possible to find pairs (Q, R) where γ has a single cycle, but the labels l_i obtained from the reverse bijection are in the wrong relative order. In other words, we may have $\zeta(\iota(Q, R)) \neq Q$.

9.2. Box math and a new statistic.

Our next approach relies on careful analysis of the poset structure on the set of rational Dyck paths under the usual inclusion relation: we say $P < Q$ if the the path P is weakly below the path Q , or, equivalently, if the set of positive hooks of P is contained in the set of positive hooks of Q . This poset is graded by the area statistic, with covering relation given by adding a single box (or equivalently, including an appropriate hook in $\mathfrak{c}(P)$). Since ζ takes skew length to co-area, it makes sense to examine what happens to the poset structure under the ζ map. The poset structure is fairly well behaved when adding or removing *maximal* hooks.

Definition 9.3. The *maximal level* m of a path P is the largest level appearing in the reading word of $L(P)$. Likewise, the *maximal box* is the outer corner of P labeled by the maximal level m . For any path with area greater than 0, we define the *predecessor* of P as the path obtained by removing the outer corner of P farthest from the diagonal. This replaces the maximal level m with $m - a - b$ in $L(P)$.

Lemma 9.4. *Suppose that P is an (a, b) -Dyck path with predecessor P' . We have $\text{sl}(P') < \text{sl}(P)$.*

Proof. Since P' is obtained by removing the maximal box of P , the laser filling of P' is equal to the laser filling of P when removing the laser filling of its maximal box. Since skew length is equal to the sum of the entries in the laser filling, the result follows. \square

Since every path has a unique maximal hook, we induce a spanning tree T in the Hasse diagram of \mathfrak{D} with the property that if $P' < P$ in T , then $\text{sl}(P') < \text{sl}(P)$.

We can also precisely describe the combinatorial effect of removing the maximal box from P on $\zeta(P)$.

Proposition 9.5. *All of the following operations are equivalent ways to remove the maximal box:*

- (1) Remove the box whose outer corner is furthest from the diagonal,
- (2) Remove the longest row from $\mathfrak{c}(P)$,
- (3) Remove the box whose associated hook length is greatest, or
- (4) In the reading word $(l_1, l_2, \dots, l_{a+b})$ of P , reduce the maximal level m by $(a+b)$, leaving all other levels unchanged.
- (5) In the standardization $\sigma(P)$, let α be the number of levels of P greater than $m - a - b$ excluding m . Replace the entry $(a+b)$ in σ with $a+b-\alpha$, and increase all entries greater than or equal to $a+b-\alpha$ by one. Equivalently, multiply $\sigma(P)$ on the left by the cycle permutation $\rho_{a+b-\alpha, a+b}$ with cycle notation $(a+b-\alpha, a+b-\alpha+1, \dots, a+b)$.
- (6) Conjugate the permutation $\gamma(P)$ by the cycle $\rho_{a+b-\alpha, a+b}$ to obtain:

$$\rho_{a+b-\alpha, a+b} \gamma(P) \rho_{a+b-\alpha, a+b}^{-1}$$

Proof. The second operation follows directly from the definition of $\mathfrak{c}(P)$. The third method is clear from inspection, and the fourth item is the effect on the relative sizes of the labels l_i of applying the third method. The fifth item follows from fourth, and the sixth item follows from the effect of conjugation on the cycle notation of a permutation. \square

We can thus try to understand the structure of the tree T by understanding certain conjugations of the permutation $\gamma(P)$.

In fact, we find it somewhat more convenient to focus on removing a maximal box from the conjugate of P . This operation corresponds to removing the maximal column from $\mathfrak{c}(P)$. The operation on paths, though, is particularly interesting.

There is good reason to consider the path P as a cycle rather than as a fixed path. For example, there is an action of the cyclic group C_{a+b} on P , obtained by rotating the last step to the start of P . The effect of this cyclic action on the labels l_i is to change all of the labels by the same fixed amount. (For example, moving a horizontal step to the front will decrease all labels by a .) This action obviously preserves the relative order of the various labels, l_i . As a result, both ζ and η are constant on the cyclic orbit. This is the underlying combinatorial reason that we consider the standardization $\sigma(P)$ as a cycle, rather than as a one-line notation.

Removing a box from a path is equivalent to finding an adjacent pair of letters NE in the path, and switching them to EN . Contrariwise, adding a box is a process of transforming an EN pair to a NE . However, when P is a Dyck path, the first step is always an N and the last step is always an E . When we consider P as a cycle, it makes sense to try exchanging this ‘adjacent’ EN pair. We can observe that (using the characterization of the conjugate of a path) that adding the box at the label $l_1 = 0$ is equivalent to removing the maximal box from P^c . This reduces all labels l_i by $a+b$ except for the label $l_1 = 0$, which remains the same. As a result, the relative value of the label 0 is increased from 1 to some number δ equal to the number of labels $l_i < a+b$, while all other labels $\leq \delta$ are reduced by one. We make this definition explicit and we have proved the following.

Definition 9.6. Define $\delta(P)$ to be the number of labels $l_i < a+b$ along P .

Proposition 9.7. *Let P' be the conjugate of the path obtained by removing the maximal box from P^c . The permutation $\gamma(P')$ is the conjugate*

$$\gamma(P') = \rho_{1, \delta(P)}^{-1} \gamma(P) \rho_{1, \delta(P)}.$$

The action of removing the maximal box from P^c on $Q = \zeta(P)$ is also completely determined by $\delta(P)$. For simplicity, we call the path $Q' = \zeta(P')$ the ζ -predecessor of Q .

Proposition 9.8. *The ζ -predecessor of $Q = \zeta(P)$ is completely determined by $\delta = \delta(P)$ as follows:*

1. All the steps in Q after the first δ steps remain unchanged.
2. The first δ steps are rotated as follows:
 - (a) the first east step that appears is changed to a north step,
 - (b) the first north step is changed to an east step,
 - (c) the first δ steps are rotated once (rotating the first step to the end of the first delta steps).

Example 9.9. An example of this procedure is illustrated in Figure 28 for the path $Q = \zeta(P)$ associated to our running example path P . The number of levels of P smaller than $a+b$ is $\delta(P) = 5$. The cycle permutation γ' is obtained from γ by rotating the labels $1, \dots, 5$. The positions of exceedences in γ are $\{1, 3, 5, 7, 9\}$ which are the positions of the north steps in Q , and the positions of exceedences in γ' are $\{1, 2, 4, 7, 9\}$ which are the positions of the north steps in Q' .

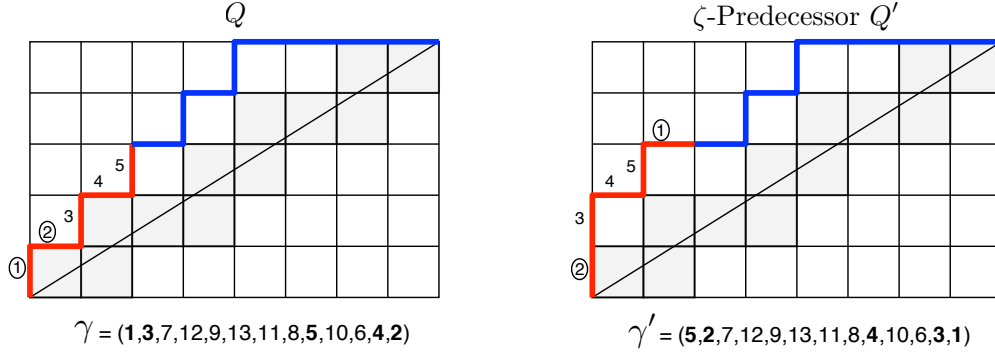


FIGURE 28. Determining the ζ -predecessor of a path $Q = \zeta(P)$ with $\delta(P)$.

Proof. As above, let P' be the conjugate of the path obtained by removing the maximal box from P^c and $Q' = \zeta(P')$ be the ζ -predecessor of Q . Let $\gamma = \gamma(P)$ and $\gamma' = \gamma(P')$, and recall that the north steps of Q and Q' are encoded by the positions of exceedences in γ and γ' respectively. The statement is equivalent to prove

1. The positions of exceedences in γ that are greater than δ are preserved and remain exceedences after rotation.
2. The positions of exceedences less than or equal to δ behave as follows:
 - (a) the position i of the first east step in Q is a non-exceedence in γ but is rotated to an exceedence at position $i - 1$ in γ' ,
 - (b) position 1 is an exceedence in γ but is rotated to a non-exceedence at position δ in γ' ,
 - (c) the positions $j \neq 1$ of exceedences in γ are rotated to positions $j - 1$ of exceedences in γ' .

These assertions follow from the description of γ' in terms of γ and δ . As illustrated in Figure 28, the cycle notation of γ' can be obtained by rotating the labels $\{1, \dots, \delta - 1, \delta\}$ to $\{\delta, 1, \dots, \delta - 1\}$ in the cycle notation of γ . Item 1 is clear from this description. Part (a) of item 2 follows from the fact that $\gamma(i) = 1$ which implies that $\gamma'(i - 1) = \delta$ (an exceedence). For this we need to argue that $i < \delta$, but this is clear since i is the relative value of the level a , which is less than $a + b$, in $L(P)$. Similarly, $\gamma(1)$ is the relative value of the level b in $L(P)$ and therefore $\gamma(1) < \delta$. Rotating the value 1, this implies that $\gamma'(\delta) = \gamma(1) - 1$ (a non-exceedence) and part (b) follows. All other positions $j \neq 1$ of exceedences less than or equal to δ in γ are clearly rotated to an exceedence at position $j - 1$ in γ' and part (c) follows. \square

Remark 9.10. The two formulations in Proposition 9.7 and Proposition 9.8 have the advantage that we do not actually need to know the value of the maximal label m , and reduces the problem of showing that ζ is a bijection to computing a single statistic. To wit, if $\delta(P)$ can be directly computed from $Q = \zeta(P)$, then we can obtain the ζ -predecessor of Q , and repeat until we arrive at the initial

path P_0 . This would completely determine P from $\zeta(P)$. To be more precise, let $Q = Q_1, \dots, Q_l$ be the list of ζ -predecessors of Q with Q_l being the final path containing all boxes above the main diagonal, and let δ_i be the δ -statistic corresponding to Q_i . The permutation $\gamma(P)$ is determined by

$$\gamma(P) = \rho \gamma_0 \rho^{-1},$$

where $\rho = \rho_{1,\delta_1} \dots \rho_{1,\delta_{l-1}}$, $\rho_{1,i}$ is the permutation with cycle notation $(1, \dots, i)$, and $\gamma_0 = \gamma(P_0)$. The east steps of the path P are encoded by the cyclic descents of γ when considered in one-line notation, as described in Section 6.1. An example of this is presented for describing the inverse of the zeta map in the Fuss-Catalan case $(a, ak + 1)$ in Section 9.4.

Corollary 9.11. *If $\delta(P)$ is determined uniquely by $\zeta(P)$ for all P , then the map ζ is invertible. In such case, the inverse path P is determined from $\gamma(P)$ as in Remark 9.10.*

Remark 9.12. The δ statistic has also been considered shortly after this paper by Xin in [Xin15a]. This statistic, and other related statistic called “key”, is used by the author to present a search algorithm for inverting the zeta map. This algorithm shows an alternative proof that the zeta map is a bijection in the Fuss-Catalan cases $(a, ak \pm 1)$, by giving a recursive construction of $\zeta^{-1}(Q)$. However, the general case remains open. The results of Xin [Xin15a] are very similar to those presented in this section, and also use the operations of removing the maximal box in P and P^c . Corollary 9.11 should be compared with [Xin15a, Corollary 19]. We also present estimates for the δ statistic and a precise formula in the Fuss-Catalan case $(a, ak + 1)$ in Proposition 9.16 and Corollary 9.18, which should be compared with [Xin15a, Theorem 16]. The estimates we present in Proposition 9.16 determine the number of children of the nodes in the search tree in the “ReciPhi algorithm” in [Xin15a, Section 5]. Our algorithm for describing the inverse of zeta in the Fuss-Catalan case $(a, ak + 1)$ in Section 9.4 should be compared with the ReciPhi algorithm for the Fuss-Catalan cases in [Xin15a, Section 5].

Remark 9.13. Computer evidence suggests that $\delta(P)$ should be computable from $\zeta(P)$. We used decision trees, a common machine learning algorithm, to try to calculate $\delta(P)$ directly from $\zeta(P)$. A *regression decision tree* attempts to take a vector v and reconstruct a function $f(v)$ by constructing a binary tree [BFSO84]. At each node of the tree, a simple comparison is made (such as $v_2 < 4.5$), with a ‘true’ result sending the computation to the right child node and a ‘false’ result sending to the left child node. The actual learning algorithm determines which comparisons to make at each level by looking at many examples to decide where the most profitable ‘split’ in the data is. For our investigations, we used the implementation of decision trees available in Scikit-Learn [PVG⁺11].

Our methodology was to fix an (a, b) pair and randomly divide the available paths into a training set consisting of 75% of the paths, and a testing set with the remaining 25%. The decision tree is trained on the training set, and testing paths are used for evaluation.

We found that decision trees were quite capable of learning to predict $\delta(P)$ for any fixed pair (a, b) we provided. For example, at $(a, b) = (17, 7)$, there are 14,421 Dyck paths. We found that the decision tree was able to exactly predict δ over 92% of the time. Treated as a regression problem, the coefficient of determination of the decision tree was greater than 0.99, indicating that the errors were also quite small. Exploration for a variety of other choices of (a, b) yielded similar results.

The decision tree is essentially treating the δ statistic as a function on the integral points of a polytope, and learning the distribution of the δ on the polytope. Our exploration indicates that the distribution of δ is well behaved, and that there may be a combinatorial algorithm for computing δ exactly.

By way of comparison, set $\psi(P)$ to be the number of peaks in P . Predicting ψ from $\zeta(P)$ is much more difficult. With $(a, b) = (17, 7)$, the decision tree’s coefficient of determination in predicting ψ is only 0.35.

As a final note, there are many possible ways to encode a Dyck path as a vector; for example, as a $\{0, 1\}$ -string with a 0’s and b 1’s, or as the partition λ which sits above the path in an $a \times b$

rectangle. For the purposes of predicting the δ statistic, we found that a most convenient encoding for $\eta(P)$ was as the values of the exceedences of $\gamma(P)$. Our decision trees allow us to see the importance of the vector coordinates in making the final prediction; in this encoding, the value of $\gamma(1)$ ends up having very high importance.

A moment's reflection shows that $\gamma(1)$ is equal to the number of labels $l_i < b$, so that $\gamma(1)$ quite directly impacts δ . Furthermore, for any $l_i < b$, we will also have an $l'_i = l_i + a < a + b$, so that $\gamma(1)$ contributes something $\leq 2\gamma(1)$ to δ (there may be some double counting here if b is much larger than a).

9.3. Initial part of a rational bounce path. The zeta map has been shown to be a bijection in the special ‘‘Fuss-Catalan’’ cases $(a, am \pm 1)$ by way of a ‘‘bounce path’’ by which zeta inverse could be computed [Loe05, GM14]. However, constructing such a bounce path for the general (a, b) case remains elusive. In this section, we construct the initial part of a rational bounce path and show its relation to the δ statistic. In particular, we explicitly compute δ in the Fuss-Catalan case $(a, ak + 1)$.

Definition 9.14. Let Q be an $(a, ak + r)$ -Dyck path with $0 \leq k$ and $0 < r < a$. The rational *initial bounce path* of Q consists of a sequence of alternating $k + 1$ *vertical moves* and k *horizontal moves*. We begin at $(0, 0)$ with a vertical move followed by a horizontal move, and continue until eventually finish with the $(k + 1)$ th vertical move. Let v_1, \dots, v_{k+1} denote the lengths of the successive vertical moves and h_1, \dots, h_k denote the lengths of the successive horizontal moves. These lengths are determined as follows.

We start from $(0, 0)$ and move north v_1 steps until reaching an east step of Q . Next, move $h_1 = v_1$ steps east. Next, move north v_2 steps from the current position until reaching an east step of Q . Next, move $h_2 = v_1 + v_2$ steps east. In general, we move north v_i steps from the current position until reaching an east step of the path, and then move east $e_i = v_1 + \dots + v_i$ steps. This is done until obtaining the last vertical move v_{k+1} .

Examples of the initial bounce path in the Fuss-Catalan case are presented in Figure 29.

Remark 9.15. The definition of the initial bounce path is exactly the same as an initial part of the bounce path in the Fuss-Catalan case [Loe05, GM14]. The description of this initial part remains the same for the general (a, b) -case but we still do not know how to extend it to a complete bounce path in general.

It turns out that the initial bounce path is closely related to the δ statistic. Denote by $|v| = v_1 + \dots + v_{k+1}$ and by $|h| = h_1 + \dots + h_k$. In all the results of this section we always assume $0 \leq k$ and $0 < r < a$.

Proposition 9.16. *Let $Q = \zeta(P)$ be an $(a, ak + r)$ -Dyck path and $\tilde{\delta}(P) \leq \delta(P)$ be the number of levels in P that are less than or equal to $a(k + 1)$. The two following equations hold:*

$$(9.1) \quad \tilde{\delta}(P) = |v| + |h| + 1,$$

$$(9.2) \quad |v| + |h| + 1 \leq \delta(P) \leq |v| + |h| + r.$$

This proposition will follow from the following lemma. Note that every such a path P contains the east levels $a, 2a, \dots, (k + 1)a$ at the end of the path. Moreover,

Lemma 9.17. *The east steps of $Q = \zeta(P)$ that are reached by the vertical moves v_1, \dots, v_{k+1} of its initial bounce path correspond to the east levels $a, 2a, \dots, (k + 1)a$ of P .*

Proof. Denote by $A_0 = \{0, 1, \dots, a - 1\}$ the set of natural numbers between 0 and $a - 1$, and let $A_i = A_0 + ia$ be the translation of A_0 by ia . Note that the number of boxes above the main diagonal that are directly on the right of a north step with north level in A_i is exactly equal to i . So, these sets can be used to encode the ‘‘area-vector’’ of a Dyck path.

As in the known Fuss-Catalan bounce path description, we will show that the vertical steps of Q that are directly on the left of the v_i vertical move contribute area $i - 1$ in P . More precisely, we will show:

1. The vertical steps of Q that are directly on the left of the v_i vertical move correspond to north levels in P that belong to A_{i-1} .
2. The horizontal steps of Q that are directly above of the h_i horizontal move correspond to east levels in P that belong to A_i .

Denote by N_i the set of north levels in P that belong to A_i , for $i = 0, \dots, k$. Similarly, denote by E_i the set of east levels in P that belong to A_i , for $i = 1, \dots, k$. We first show that E_i can be obtained as the disjoint union

$$(9.3) \quad E_i = \bigcup_{j=0}^{i-1} (N_j + (i-j)a).$$

For this, note that the first north level in P that appears after an east level $e \in E_i$ should be a north level $n \in N_j$ for some $j \in \{0, \dots, i-1\}$, and that $e = n + (i-j)a$. Reciprocally, every north level $n \in N_j$ for some $j \in \{0, \dots, i-1\}$ forces the east levels $e_{j+1}, e_{j+2}, \dots, e_k$ to appear as east levels in P , where $e_{j+l} = n + la$ (indeed, $e_{j+l} \in A_{j+l}$ which means that $e_{k-1} < ak < b = ak + r$. Then, all the lattice points one step below $e_{j+1}, e_{j+2}, \dots, e_{k-1}$ are below the main diagonal). Thus, the north level $n \in N_j$ contributes with exactly one east level $e = n + (i-j)a$ in E_i .

Items 1 and 2 above are now equivalent to prove that $v_i = |N_{i-1}|$ and $h_i = |E_i|$. Equation 9.3 implies that $|E_i| = |N_0| + \dots + |N_{i-1}|$. Since $h_i = v_1 + \dots + v_i$, it suffices to prove $v_i = |N_{i-1}|$. Note that v_1 is clearly the number of elements in N_0 , since the smallest east level of P (which corresponds to the first east step in Q) is equal to a . Moving $h_1 = v_1 = |E_1|$ steps horizontally covers all the east steps of Q corresponding to the east levels in P that belong to A_1 . Moving up v_2 units from the current position hits the path at the east step corresponding to the first east level of P that belongs to A_2 . This east level is exactly equal to $2a$, and all the north steps on the left of v_2 in Q correspond to the north levels in P that belong to A_1 , that is $v_2 = |N_1|$. In general, P contains all east levels $a, 2a, \dots, (k+1)a$. Therefore, the initial value of E_i is equal to ia and is smaller than all values in N_i . As a consequence the vertical move v_i of the bounce path hits the path Q precisely at the east step corresponding to the level ia of P as desired, and $v_i = |N_{i-1}|$. This finishes the proof of the proposition and the proof of items 1 and 2. \square

Proof of Proposition 9.16. The east step of Q that is reached by the vertical move v_{k+1} corresponds to the east level $(k+1)a$ in P . So, $\tilde{\delta}(P)$ is equal to the position of this east step in Q , which is equal to $|v| + |h| + 1$. Since $a + b = (k+1)a + r$ and $a + b$ never appears as a level in P , then $\delta \leq \tilde{\delta} + r - 1 = |v| + |h| + r$. \square

Replacing $r = 1$ in Equation (9.2), we obtain.

Corollary 9.18. *In the Fuss-Catalan case $(a, ak+1)$, the statistic $\delta(P)$ is determined by the initial bounce path of $Q = \zeta(P)$ by*

$$(9.4) \quad \delta(P) = |v| + |h| + 1.$$

9.4. Inverse of zeta in the Fuss-Catalan case $(a, ak+1)$. As a consequence of Corollary 9.11 and Corollary 9.18 we obtain an alternative proof that the zeta map is a bijection in the Fuss-Catalan case $(a, ak+1)$, as previously shown by Loehr in [Loe05]. Our approach is similar to the algorithmic approach of Xin in [Xin15a].

Corollary 9.19. *The zeta map is a bijection in the Fuss-Catalan case $(a, ak+1)$.*

Moreover, Remark 9.10 gives us a precise simple way for computing the inverse of zeta of a path Q . We describe this procedure by means of an example below. Let $Q = NENEENEEEE$

be the $(3, 7)$ Fuss-Catalan path illustrated in Figure 29. In order to compute $\zeta^{-1}(Q)$ we find the list of ζ -predecessors $Q = Q_1, Q_2, \dots, Q_l$ of Q until arriving to the final path Q_l containing all the boxes above the main diagonal. Let δ_i be the δ statistic corresponding to the path Q_i , which can be computed from the initial bounce path of Q_i as $|v| + |h| + 1$. The path Q_{i+1} is obtained from Q_i using Proposition 9.8. Equivalently, Q_{i+1} is obtained from Q_i by “moving” all the north steps on the left of its initial bounce path one step to the left whenever possible, as illustrated in Figure 29. The inverse of zeta of the final path Q_l is the initial diagonal path P_0 . Let $\gamma_0 = \gamma(P_0)$ be its corresponding cycle permutation, which can be computed either directly from P_0 or from the pair (Q_l, Q_l) using the description of ι in Section 6.1. In our example,

$$\gamma_0 = (1, 8, 5, 2, 9, 6, 3, 10, 7, 4).$$

If $P = \zeta^{-1}(Q)$, the permutation $\gamma(P)$ is determined by

$$\gamma(P) = \rho \gamma_0 \rho^{-1},$$

where $\rho = \rho_{1, \delta_1} \dots \rho_{1, \delta_{l-1}}$ and $\rho_{1, i}$ is the permutation with cycle notation $(1, \dots, i)$. In our example,

$$\rho = (1, \dots, 7)(1, \dots, 9)(1, \dots, 9) = [4, 5, 6, 7, 1, 8, 9, 2, 3, 10],$$

and

$$\begin{aligned} \gamma(P) &= (4, 2, 1, 5, 3, 8, 6, 10, 9, 7) \\ &= (1, \mathbf{5}, 3, \mathbf{8}, 6, \mathbf{10}, \mathbf{9}, \mathbf{7}, \mathbf{4}, \mathbf{2}). \end{aligned}$$

Replacing the cyclic descents of $\gamma(P)$ (when considered in one-line notation) by east steps and the ascents by north steps we recover the path $\zeta^{-1}(Q) = P = \mathbf{NENENE} \mathbf{EEEE}$. We have computed the image of P under the zeta map in Figure 30 to verify that it is indeed equal to Q .

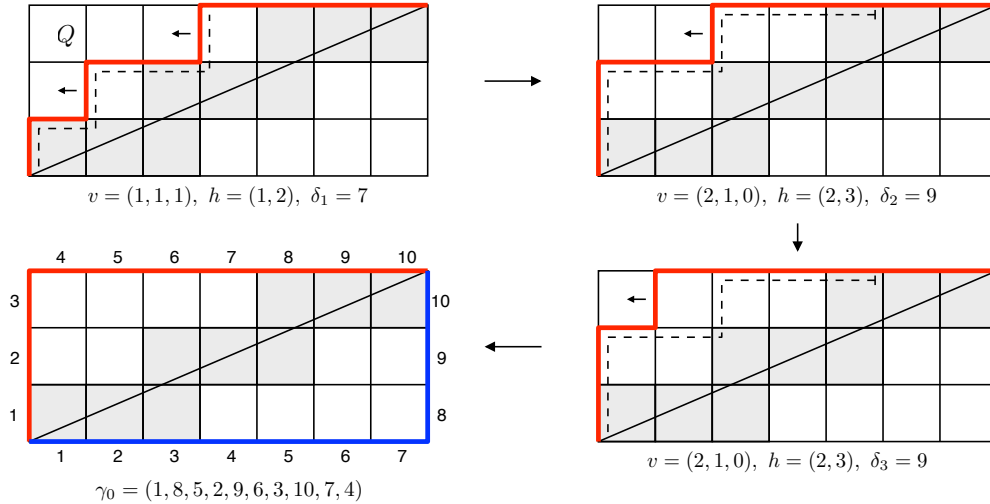
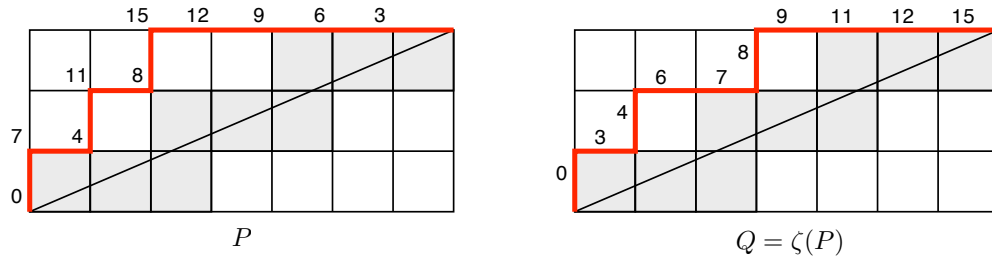


FIGURE 29. ζ -predecessors and corresponding δ statistics of a Fuss-Catalan path Q . The dotted lines are the corresponding initial bounce paths. $\zeta^{-1}(Q)$ is the path whose east steps correspond to the cyclic descents of the permutation γ , obtained by conjugating γ_0 by the cycles ρ_{1, δ_i} .

ACKNOWLEDGEMENTS

Some of the results in this work are partially the result of working sessions at the Algebraic Combinatorics Seminar at the Fields Institute with the active participation of Farid Aliniaiefard, Nantel Bergeron, Eric Ens, Sirous Homayouni, Sahar Jamali, Shu Xiao Li, Trueman MacHenry, and


 FIGURE 30. Verification of $\zeta^{-1}(Q) = P$.

Mike Zabrocki. The connection with the Fibonomial and FiboCatalan numbers in Remark 3.10 is also a result of this seminar and is further explored in forthcoming work [ABCL15], we also thank Bruce Sagan for useful discussions and exchange of ideas related to that.

We specially thank Rishi Nath for discussions involving core partitions that helped simplify arguments in Section 3, Drew Armstrong for sharing his knowledge of the history of this subject, and Greg Warrington for pointing us the references about the div statistic in Remark 5.4. We are also grateful to York University for hosting a visit of the third author.

REFERENCES

- [ABCL15] Farid Aliniaefard, Nantel Bergeron, Cesar Ceballos, and Shu Xiao Li, *q-analogs of the Fibonomial and FiboCatalan numbers*, In preparation, 2015.
- [AHJ14] Drew Armstrong, Christopher R. H. Hanusa, and Brant C. Jones, *Results and conjectures on simultaneous core partitions*, European Journal of Combinatorics **41** (2014), 205–220.
- [ALW14a] Drew Armstrong, Nicholas A. Loehr, and Gregory S. Warrington, *Rational parking functions and Catalan numbers*, Preprint: <http://arxiv.org/abs/1403.1845>, 2014.
- [ALW14b] ———, *Sweep maps: A continuous family of sorting algorithms*, Preprint: <http://arxiv.org/abs/1406.1196>, 2014.
- [And02] Jaclyn Anderson, *Partitions which are simultaneously t_1 - and t_2 -core*, Discrete Math. **248** (2002), 237–243.
- [ARW13] Drew Armstrong, Brendon Rhoades, and Nathan Williams, *Rational associahedra and noncrossing partitions*, Electron. J. Combin. **20** (2013), no. 3, P54.
- [BFSO84] Leo Breiman, Jerome Friedman, Charles J. Stone, and Richard A. Olshen, *Classification and regression trees*, CRC press, 1984.
- [BGLX14] Francois Bergeron, Adriano Garsia, Emily Leven, and Guoce Xin, *Compositional (km, kn) -shuffle conjectures*, Preprint: <http://arxiv.org/abs/1404.4616>, 2014.
- [Biz54] M. T. L. Bizley, *Derivation of a new formula for the number of minimal lattice paths from $(0, 0)$ to (km, kn) having just t contacts with the line $my = nx$ and having no points above this line; and a proof of Grossmans formula for the number of paths which may touch but do not rise above this line.*, Journal of the Institute of Actuaries (1954), no. 80, 55–62.
- [DM47] A. Dvoretzky and Th. Motzkin, *A problem of arrangements*, Duke Math. J. **14** (1947), 305–31.
- [GG12] Iain G. Gordon and Stephen Griffeth, *Catalan numbers for complex reflection groups*, American Journal of Mathematics **134** (2012), no. 6, 1491–1502. MR 2999286
- [GM13] Evgeny Gorsky and Mikhail Mazin, *Compactified Jacobians and -Catalan numbers, I*, Journal of Combinatorial Theory, Series A **120** (2013), no. 1, 49–63.
- [GM14] ———, *Compactified Jacobians and q, t -Catalan numbers, II*, J. Algebraic Combin. **39** (2014), no. 1, 153–186 (English).
- [GMV14] Evgeny Gorsky, Mikhail Mazin, and Monica Vazirani, *Affine permutations and rational slope parking functions*, To appear, Transactions of the American Mathematical Society (2014), Preprint: <http://arxiv.org/abs/1403.0303>.
- [Hag08] J Haglund, *The q, t -Catalan numbers and the space of diagonal harmonics, with an appendix on the combinatorics of Macdonald polynomials, university lecture series, 41*, American Mathematical Society, Providence, RI (2008).
- [Hai94] Mark D. Haiman, *Conjectures on the quotient ring by diagonal invariants*, J. Algebraic Combin. **3** (1994), no. 1, 17–76. MR 1256101 (95a:20014)

- [KL14] Ryan Kaliszewski and Huilan Li, *The symmetry of the (m, n) -rational q, t -Catalan numbers for $m = 3$* , Preprint: <http://arxiv.org/abs/1412.3475>, 2014.
- [LM05] Luc Lapointe and Jennifer Morse, *Tableaux on $k + 1$ -cores, reduced words for affine permutations, and k -Schur expansions*, J. Combin. Theory Ser. A **112** (2005), no. 1, 44–81. MR 2167475 (2006j:05214)
- [Loe05] Nicholas A. Loehr, *Conjectured statistics for the higher q, t -Catalan sequences*, Electron. J. Combin. **12** (2005), Research Paper 9, 54. MR 2134172 (2006e:05010)
- [LW09] Nicholas A. Loehr and Gregory S. Warrington, *A continuous family of partition statistics equidistributed with length*, Journal of Combinatorial Theory, Series A **116** (2009), no. 2, 379–403.
- [Ols93] Jørn B. Olsson, *Combinatorics and representations of finite groups*, ii+94. MR 1264418 (95b:20020)
- [PVG⁺11] F. Pedregosa, G. Varoquaux, A. Gramfort, V. Michel, B. Thirion, O. Grisel, M. Blondel, P. Prettenhofer, R. Weiss, V. Dubourg, J. Vanderplas, A. Passos, D. Cournapeau, M. Brucher, M. Perrot, and E. Duchesnay, *Scikit-learn: Machine learning in Python*, Journal of Machine Learning Research **12** (2011), 2825–2830.
- [SS10] Bruce Sagan and Carla Savage, *Combinatorial interpretations of binomial coefficient analogues related to Lucas sequences*, EJCNT **10** (2010), 697–703.
- [ST14] Robin Sulzgruber and Marko Thiel, *Type c parking functions and a zeta map*, Preprint: <http://arxiv.org/abs/1411.3885>, 2014.
- [Xin15a] Guoce Xin, *An efficient search algorithm for inverting the sweep map on rational Dyck paths*, Preprint: <http://arxiv.org/abs/1505.00823>, 2015.
- [Xin15b] ———, *Rank complement of rational Dyck paths and conjugation of (m, n) -core partitions*, Preprint: <http://arxiv.org/abs/1504.02075>, 2015.

DEPARTMENT OF MATHEMATICS AND STATISTICS, YORK UNIVERSITY, TORONTO, ONTARIO M3J 1P3, CANADA
E-mail address: ceballos@mathstat.yorku.ca
URL: <http://garsia.math.yorku.ca/~ceballos/>

DEPARTMENT OF MATHEMATICS AND STATISTICS, YORK UNIVERSITY, TORONTO, ONTARIO M3J 1P3, CANADA
E-mail address: sdenton4@gmail.com
URL: <http://inventingsituations.net/>

DEPARTMENT OF MATHEMATICS, QUEENS COLLEGE (CUNY), 65-30 KISSENA BLVD., FLUSHING, NY 11367
E-mail address: chanusa@qc.cuny.edu
URL: <http://qc.edu/~chanusa/>